Supporting Information for

Circularly Polarized Luminescence from Helical N,O-Boron-Chelated Dipyrromethenes (BODIPY) Derivatives

Ling-Yun Wang, Zheng-Fei Liu, Kun-Xu Teng, Li-Ya Niu* and Qing-Zheng Yang*

Key Laboratory of Radiopharmaceuticals, Ministry of Education, College of Chemistry, Beijing Normal University, Beijing 100875, P. R. China.

Content

1. Materials and instruments

Unless otherwise mentioned, the reagents and solvents are of commercial quality and were used without further purification. Column chromatography was performed over silica gel (200-300 mesh) ^{1}H and ^{13}C NMR spectra were recorded on JEOL-400 or JEOL-600 spectrometer using tetramethyl silane (TMS) as internal standard at room temperature and referenced to solvent signals. Mass spectra were obtained on a Thermo Fisher Q-Exactive or Bruker Solarix XR Fourier Transform Ion Cyclotron Resonance Mass Spectrometer. Fluorescence spectra were determined on Hitachi 4500 spectrophotometer. Absorption

spectra were determined on Hitachi UV-3900 spectrophotometer. Fluorescence quantum yields were determined on HAMAMATSU C11347. The lifetime was determined on Edinburgh LP 980 spectrometer. The values of lifetime were analyzed by exponential function fitting with software F900. Chiral high-performance liquid chromatography (HPLC) separation was performed by WuXi AppTec company. Circular dichroism (CD) spectra were obtained by using CD spectra were recorded on a Chirascan™ Circular Dichroism spectrometer (Applied Photophysics Ltd, Surrey, United Kingdom). Circularly polarized luminescence measurements and DC (nonpolarized fluorescence) signals were performed with a JASCO CPL-300 spectrometer. Single crystal X-Ray diffraction data were collected at 100 K with a SuperNova Rigaku Oxford Diffraction diffractometers with Cu−Kα radiation, λ = 1.54184 Å. Fluorescence microscope images were performed on OLYMPUS IXTI. In SEM studies, the samples were centrifuged and washed by deionized water twice to remove the interference of surfactants. The samples were examined after Au spraying with Hitachi SU8010 at an accelerating voltage of 5 or 10 kV.

2. Synthesis and Characterization

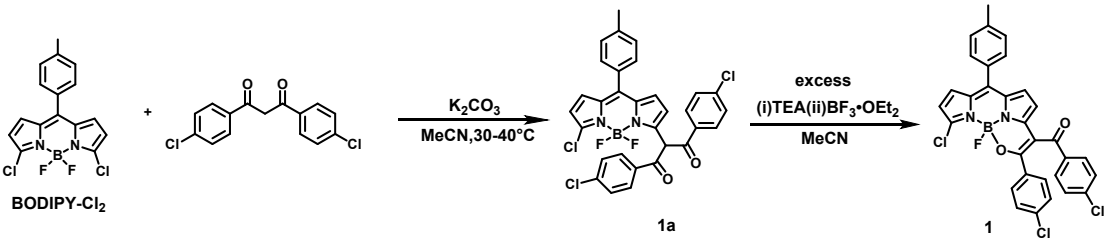

Compound **BODIPY-Cl_2** was synthesized according to the reported methods.[1]

Compound **1** was synthesized according to the reported methods. [2] The synthesis of compound **1a** was optimized using K_2CO_3 instead of NaH. The detailed procedures are as followed:

Synthesis of compound **1a: BODIPY-Cl_2** (176 mg, 0.5 mmol) was dissolved in dry acetonitrile (30 mL). 1,3-bis(4-chlorophenyl)propane-1,3-dione (146 mg, 0.5 mmol) and K_2CO_3 (0.69 g, 5 mmol) were added. The reaction mixture was stirred at room temperature for 2~3 h, and then water was added to quench the reaction. The mixture was extracted with dichloromethane. The organic layer was dried over $MgSO_4$, and the solvent was removed under reduced pressure. The crude product was purified through column chromatography over silica (dichloromethane / petroleum ether = 1/1 as eluent) to give **2a** (173 mg, 55%) as a red solid.

1 was separated by chiral high-performance liquid chromatography (HPLC) to afford a pair of optically stable enantiomers named **P1** and **M1.**

Column: (S,S)-WHELK-O1, 100×4.6 mm, 3.5 um.

Mobile phase: A: CO2, B: EtOH (0.05%DEA), Gradient: from 10% to 40% in 2 min and hold 40%for 2min, then from 40% to 10% in 0.7min, hold 10% 0.8min Flow rate: 2.5 mL/min. Column temperature: 35 °C. ABPR: 1500psi.

P1: ^{1}H NMR (600 MHz, Chloroform-*d*) δ 7.73 – 7.67 (m, 2H), 7.62 (d, *J* = 8.8 Hz, 2H), 7.50 (d, *J* = 7.8 Hz, 2H), 7.34 (d, *J* = 7.8 Hz, 2H), 7.20 (d, *J* = 8.1 Hz, 4H), 7.09 (q, *J* = 4.5 Hz, 2H), 6.91 (d, *J* = 4.4 Hz, 1H), 6.47 (d, *J* = 4.4 Hz, 1H), 2.48 (s, 3H). ^{13}C NMR (151 MHz, CHLOROFORM-*d*) δ 192.90, 165.07, 152.24, 140.79, 139.45, 139.04, 137.65, 136.54, 135.53, 134.08, 133.40, 132.62, 131.99, 131.46, 130.80, 130.23, 130.19, 129.19, 128.41, 128.29, 125.99, 119.54, 115.10, 21.24. ESI-HRMS: calculated for [M+H] $^+$

569.0581, found 569.0559.

M1: ^{1}H NMR (400 MHz, Chloroform-*d*) δ 7.69 (d, *J* = 6.1 Hz, 2H), 7.62 (d, *J* = 7.4 Hz, 2H), 7.55 – 7.47 (m, 2H), 7.35 (d, *J* = 7.7 Hz, 2H), 7.20 (d, *J* = 7.8 Hz, 4H), 7.13 – 7.06 (m, 2H), 6.91 (d, *J* = 4.1 Hz, 1H), 6.47 (d, *J* = 4.2 Hz, 1H), 2.48 (s, 3H). ^{13}C NMR (151 MHz, CHLOROFORM-*D*) δ 192.91, 165.08, 152.25, 140.80, 139.46, 139.05, 137.66, 136.54, 135.54, 134.08, 133.41, 132.62, 132.00, 131.46, 130.81, 130.24, 130.19, 129.20, 128.42, 128.29, 126.00, 119.54, 115.11, 21.24. ESI-HRMS: calculated for [M+H] $^{+}$ 569.0581, found 569.0585.

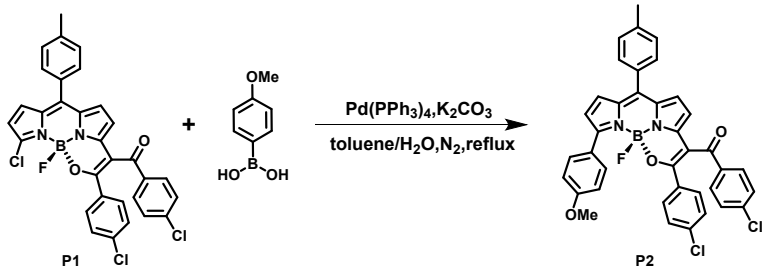

Synthesis of **P2**: $Pd(PPh3)_4$ (0.004 mmol, 0.004 g), and 4-methoxyphenylboronic acid (0.074mmol, 12 mg) were added to the solution of **P1** (0.068 mmol, 40 mg) in toluene under nitrogen. Then aqueous K_2CO_3 (1 M, 0.4 mmol, 0.4 mL) was added through a syringe. The reaction mixture was heated under reflux for 2h. The reaction was monitored by TLC, after the raw material disappeared, the solution was extracted with dichloromethane and washed with brine. The organic solution was dried over anhydrous sodium sulfate and evaporated under reduced pressure. The residue was purified by chromatography on silica gel with petroleum ether/dichloromethane (100:25, v/v) as an eluent to give the compound **M2** (25mg, 56% yield) dark-green solid. ^{1}H NMR (600 MHz, Chloroform-*d*) δ 7.99 (d, *J* = 8.6 Hz, 2H), 7.66 (d, *J* = 8.4 Hz, 2H), 7.54 (d, *J* = 7.5 Hz, 2H), 7.34 (d, *J* = 7.7 Hz, 2H), 7.28 (d, *J* = 8.2 Hz, 2H), 7.18 (d, *J* = 7.8 Hz, 2H), 7.04 (d, *J* = 8.4 Hz, 4H), 7.02 (d, *J* = 4.5 Hz, 1H), 6.98 (d, *J* = 4.0 Hz, 1H), 6.94 (d, *J* = 4.3 Hz, 1H), 6.61 (d, *J* = 4.0 Hz, 1H), 3.93 (s, 3H), 2.48 (s, 3H). ^{13}C NMR (151 MHz, CHLOROFORM-D) δ 193.53, 163.80, 160.76, 154.15, 150.52, 140.80, 140.70, 139.20, 137.51, 137.44, 137.05, 134.00, 132.19, 131.79, 131.51, 131.15, 130.82, 130.64, 130.58, 129.40, 128.69, 128.21, 125.88, 118.29, 118.18, 113.96, 109.81, 55.60, 21.60. ESI-HRMS: calculated for $[M+H]^{+}$ 659.1477, found 659.1472.

Synthesis of **M2**: The synthetic procedure is the same as the **P2**, just replaced **P2** with **M2**. ^{1}H NMR (600 MHz, Chloroform-d) δ 7.99 (d, *J* = 8.3 Hz, 2H), 7.66 (d, *J* = 7.9 Hz, 2H), 7.54 (d, *J* = 7.4 Hz, 2H), 7.35 (d, *J* = 7.5 Hz, 2H), 7.28 (d, *J* = 8.0 Hz, 2H), 7.18 (d, *J* = 7.9 Hz, 2H), 7.04 (d, *J* = 8.2 Hz, 4H), 7.02 (d, *J* = 4.5 Hz, 1H), 6.98 (d, *J* = 3.9 Hz, 1H), 6.93 (d, *J* = 4.2 Hz, 1H), 6.61 (d, *J* = 4.0 Hz, 1H), 3.93 (s, 3H), 2.48 (s, 3H). ^{13}C NMR (151 MHz, CHLOROFORM-D) δ 193.54, 163.81, 160.76, 154.15, 150.53, 140.81, 140.71, 139.21, 137.51, 137.45, 137.05, 134.00, 132.20, 131.79, 131.51, 131.15, 130.83, 130.64, 130.59, 129.41, 128.70, 128.22, 125.88, 118.30, 118.18, 113.97, 109.81, 76.95, 55.61, 21.61. ESI-HRMS: calculated for $[M+H]^{+}$ 659.1477, found 659.1480.

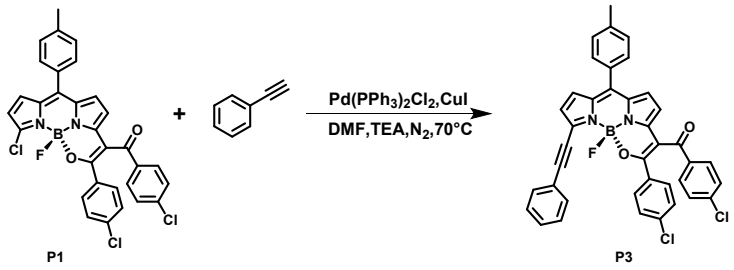

Synthesis of **P3**: $Pd(PPh3)_2Cl_2$ (0.004 mmol, 2.4 mg) and Copper(I) iodide (0.004 mmol, 1 mg) were added to the solution of **P1** (0.068 mmol, 40 mg) in N,N-dimethylformamide (DMF, 1.5 mL) under nitrogen. Then, phenylacetylene (0.075 mmol, 8 μL) and triethylamine (0.5 mL) were added to the resulting mixture through a syringe. The reaction mixture was heated at 75 °C for 2 h. The reaction was monitored by TLC, after the raw material disappeared, the product was extracted with ethyl acetate and the organic layers were combined and washed with H_2O (5×30 mL). The organic solution was dried over anhydrous sodium sulfate and evaporated under reduced pressure. The residue was purified by chromatography on silica gel with petroleum ether/dichloromethane (100:10, v/v) as an eluent to give the compound **M3** (22 mg, 50% yield) as dark-green solid .^{1}H NMR (400 MHz, Chloroform-*d*) δ 7.69 (d, *J* = 8.5 Hz, 2H), 7.63 (d, *J* = 6.0 Hz, 2H), 7.53 (d, *J* = 8.3 Hz, 4H), 7.44 (t, *J* = 7.2 Hz, 3H), 7.35 (d, *J* = 7.9 Hz, 2H), 7.20 (d, *J* = 8.5 Hz, 2H), 7.10 (d, *J* = 4.6 Hz, 1H), 7.05 (d, *J* = 4.6 Hz, 1H), 6.97 – 6.90 (m, 3H), 6.82 (d, *J* = 4.1 Hz, 1H), 2.49 (s, 3H). ^{13}C NMR (151 MHz, CHLOROFORM-*D*) δ 193.28, 165.78, 152.92, 141.00, 139.37, 139.24, 137.70, 136.99, 136.41, 133.90, 132.42, 132.21, 131.94, 131.20, 130.66, 130.25, 129.54, 129.29, 128.78, 128.56, 128.39, 125.64, 122.81, 121.97, 120.05, 109.66, 97.51, 83.21, 21.62. ESI-HRMS: calculated for $[M+H]^+$ 633.1309, found 633.1304

Synthesis of **M3**: The synthetic procedure is the same as the **P3**, just replaced **P3** with **M3**. ^{1}H NMR (600 MHz, Chloroform-d) δ 7.69 (d, *J* = 8.2 Hz, 2H), 7.63 (d, *J* = 7.5 Hz, 2H), 7.54 (s, 4H), 7.44 (dt, *J* = 13.9, 6.9 Hz, 3H), 7.35 (d, *J* = 7.8 Hz, 2H), 7.20 (d, *J* = 8.2 Hz, 2H), 7.10 (d, *J* = 4.6 Hz, 1H), 7.05 (d, *J* = 4.5 Hz, 1H), 6.97 – 6.91 (m, 3H), 6.82 (d, *J* = 4.2 Hz, 1H), 2.48 (s, 3H). ^{13}C NMR (151 MHz, Chloroform-*d*) δ 193.13, 165.62, 152.75, 140.84, 139.21, 139.08, 137.54, 136.83, 136.24, 133.73, 132.26, 132.06, 131.79, 131.04, 131.03, 130.50, 130.08, 129.38, 129.13, 128.62, 128.40, 128.23, 125.48, 122.64, 121.81, 119.89, 109.49, 97.35, 83.05, 21.46. ESI-HRMS: calculated for $[M+H]^+$ 633.1309, found 633.1302.

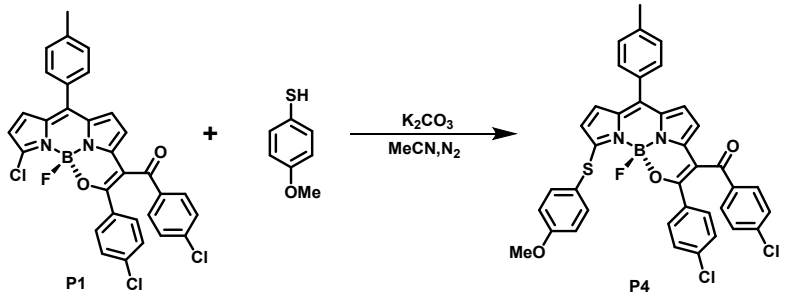

Synthesis of **P4**: Compound **P1** (0.051 mmol, 30mg) was dissolved in dry acetonitrile, then 4-methoxybenzenethiol (0.1 mmol, 14 mg) and K_2CO_3 (0.7 mmol, 100 mg) were added

under nitrogen. The mixture was stirred at room temperature for 2 h, the reaction was monitored by TLC, after the raw material disappeared, the solution was evaporated. The residue was purified by chromatography on silica gel (dichloromethane / petroleum ether = 100:10, v/v) to give the compound **M4** (16 mg, 45% yield) as dark-green solid. ^{1}H NMR (400 MHz, Chloroform-*d*) δ 7.73 (d, *J* = 8.6 Hz, 2H), 7.68 (d, *J* = 8.6 Hz, 2H), 7.64 (d, *J* = 8.9 Hz, 2H), 7.49 (d, *J* = 8.0 Hz, 2H), 7.31 (d, *J* = 7.9 Hz, 2H), 7.20 (d, *J* = 8.5 Hz, 4H), 7.03 – 6.94 (m, 4H), 6.89 (d, *J* = 4.4 Hz, 1H), 5.95 (d, *J* = 4.3 Hz, 1H), 3.86 (s, 3H), 2.46 (s, 3H). ^{13}C NMR (101 MHz, CHLOROFORM-D) δ 193.83, 163.52, 161.18, 154.06, 148.97, 140.64, 139.23, 138.60, 137.37, 137.09, 137.01, 134.09, 131.73, 131.26, 130.56, 129.87, 129.43, 128.71, 128.54, 127.89, 120.32, 117.47, 117.01, 115.43, 109.74, 55.61, 21.58. ESI-HRMS: calculated for $[M+H]^+$ 671.1136, found 671.1139.

Synthesis of **M4**: The synthetic procedure is the same as the **P4**, just replaced **P4** with **M4**. ^{1}H NMR (400 MHz, Chloroform-*d*) δ 7.73 (d, *J* = 8.6 Hz, 2H), 7.68 (d, *J* = 8.6 Hz, 2H), 7.64 (d, *J* = 8.9 Hz, 2H), 7.49 (d, *J* = 8.0 Hz, 2H), 7.31 (d, *J* = 7.9 Hz, 2H), 7.20 (d, *J* = 8.6 Hz, 4H), 7.04 – 6.95 (m, 4H), 6.89 (d, *J* = 4.3 Hz, 1H), 5.95 (d, *J* = 4.2 Hz, 1H), 3.86 (s, 3H), 2.46 (s, 3H). ^{13}C NMR (151 MHz, CHLOROFORM-D) δ 193.81, 163.53, 161.20, 154.03, 149.03, 140.63, 139.24, 138.61, 137.40, 137.37, 137.13, 136.98, 134.13, 131.73, 131.27, 130.56, 129.87, 129.43, 128.71, 128.54, 127.88, 120.40, 117.50, 117.05, 115.44, 109.77, 55.61, 21.57. ESI-HRMS: calculated for $[M+H]^+$ 671.1136, found 671.1141.

3. Analysis of the enantiomer excess.

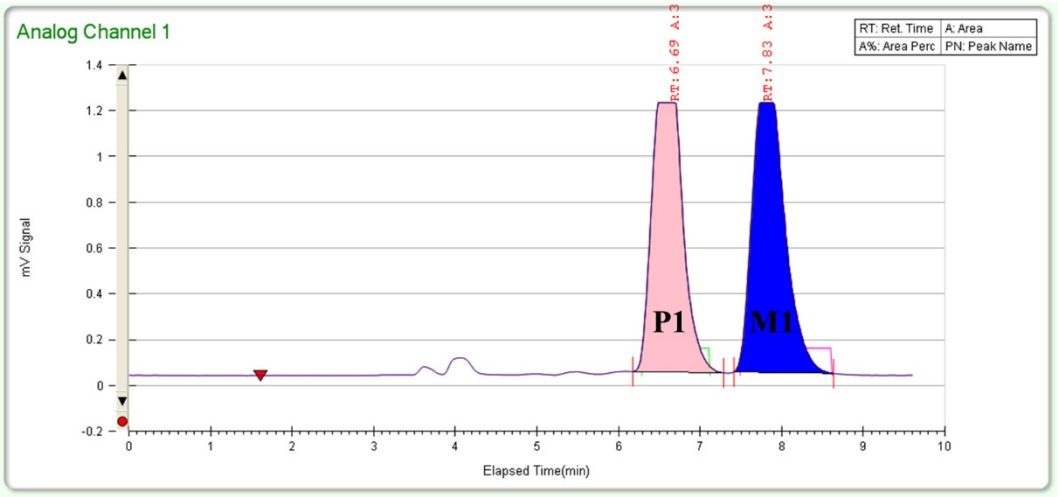

Fig. S1. HPLC separation profile of Compound **1** for 10 min.

Table S1. The summary of HPLC profiles of **1** for 10 min.

Compound	Peak	RT	Area	Area %	Height
1	1	4.139	515803	48.77	91338
	2	5.011	541914	51.23	65811

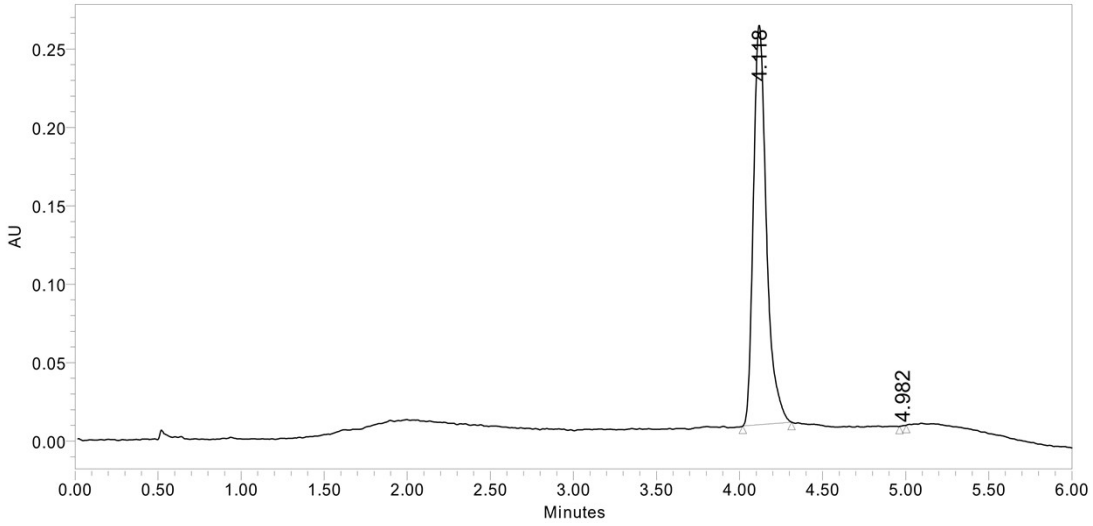

Fig. S2. HPLC profile of **P1** for 6 min.

Table S2. The summary of HPLC profiles of **P1** for 6 min.

Compound	Peak	RT	Area	Area %	Height	ee value
P1	1	4.118	1392840	99.99	254786	99.98
	2	4.982	127	0.01	105	

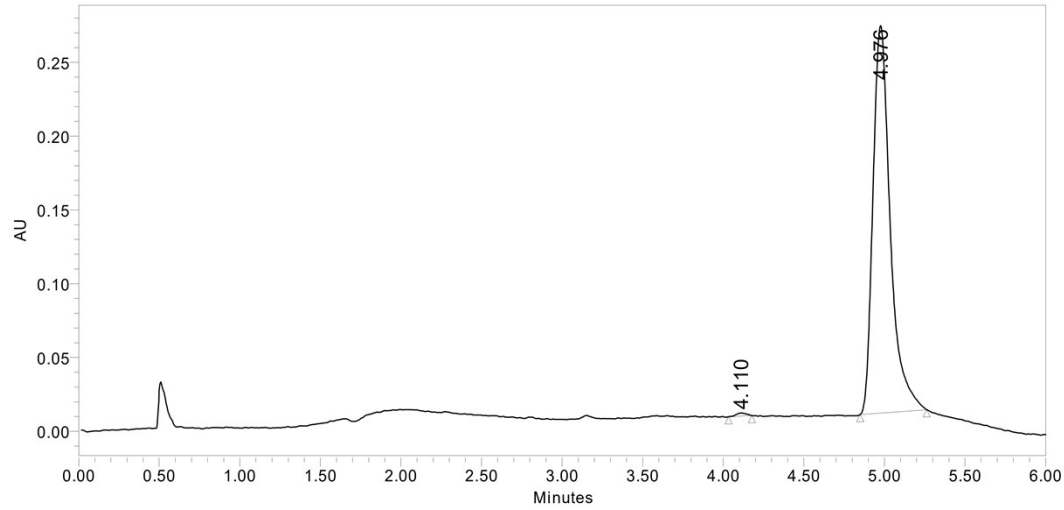

Fig. S3. HPLC profile of **M1** for 6 min.

Table S3. The summary of HPLC profiles of **M1** for 6 min.

Compound	Peak	RT	Area	Area %	Height	ee value
M1	1	4.110	8964	0.45	2079	99.10
	2	4.976	1962101	99.55	262559	

4. Crystallographic data of 1, P1 and P3/M3.

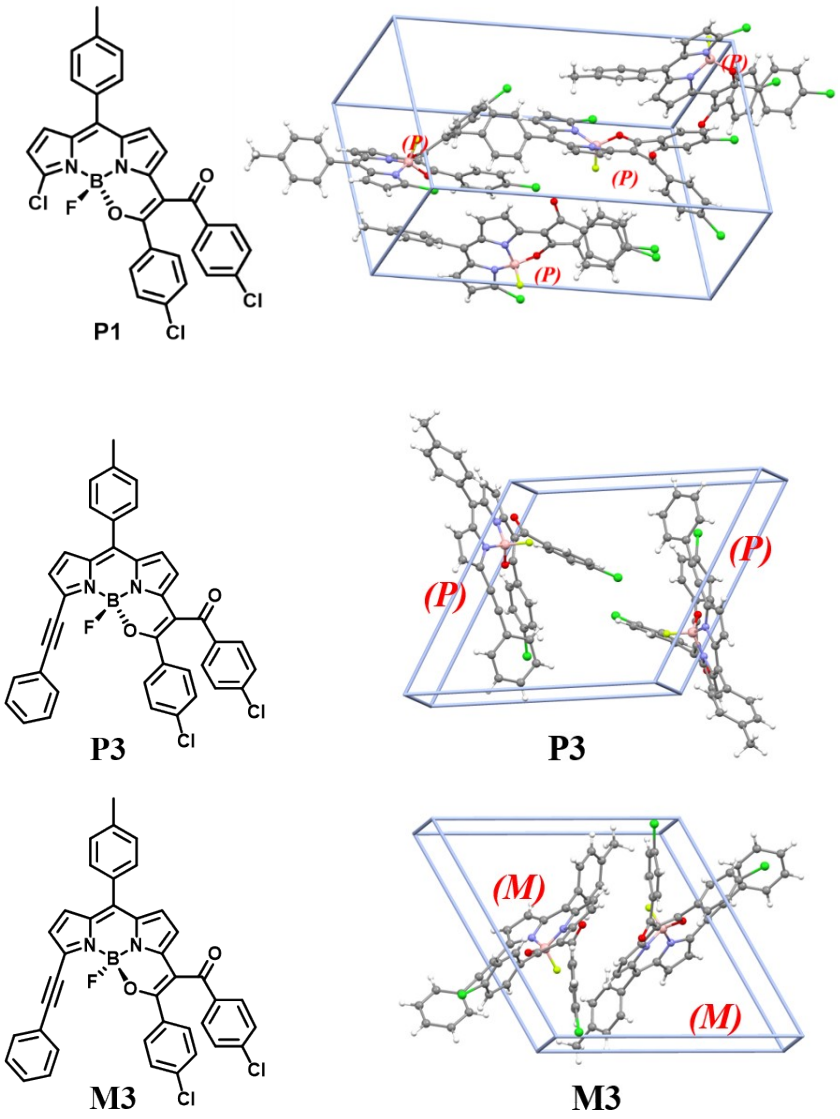

Fig. S4. The chemical and single crystal structure of **P1, P3** and **M3** (labeled by the absolute configuration).

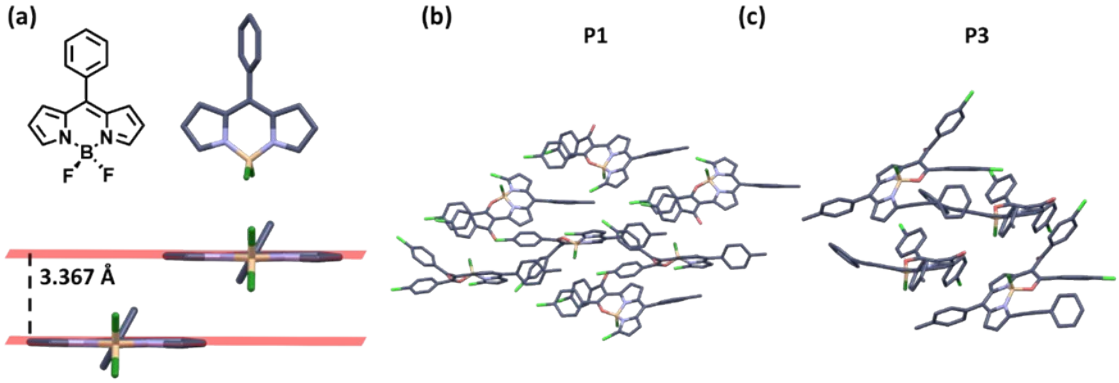

Fig. S5. The stacking structures of (a) a conventional BODIPY, (b) **P1** and (c) **P3**. All hydrogen atoms are omitted for clarity. The BODIPY cores of **P1** and **P3** are exhibit in

spacefill style for clarity.

In Fig. S5, the stacking structures of helical BODIPYs are compared with conventional planar BODIPY. As for conventional BODIPY, there is close π···π stacking in crystal, the stacking distance is 3.367 Å. In contrast, there are almost no overlap between BODIPY cores in **P1** and **P3** crystals.

Table S4. Crystal data and structure refinement for **1**

	1
CCDC number	1830265
Empirical formula	$C_{31}H_{19}BN_2O_2FCl_3$
Formula weight	587.64
Temperature/K	150.0
Crystal system	Triclinic
Space group	P-1
Unit cell dimensions	a = 9.8835 (4) Å b = 10.9565 (4) Å c = 13.9024 (6) Å α = 98.465(3)° β = 109.164(4)° γ = 105.933(4)°
Volume (Å3)	1319.91(10)
Z	2
ρcalc g/cm3	1.479
μ/mm-1	3.487
F(000)	600.0
Crystal size/mm^3	0.15 × 0.15 × 0.05
Radiation	CuKα (λ = 1. 54184)
2Θ range for data collection/o	4.3400 to 73.1130
Index ranges	-12 ≤ h ≤ 11, -10 ≤ k ≤ 13, -17 ≤ l ≤ 16
Reflections collected	9023
Independent reflections	5135 [Rint = 0.0214, Rsigma = 0.0292]
Data/restraints/parameters	5135/0/362
Goodness-of-fit on F2	1.023
Final R indices [I>2sigma(I)]	R1 = 0.0338, wR2 = 0.0859
Rindices (all data)	R1 = 0.0379 wR2 = 0.0897
Largest diff. peak/hole / e Å-3	0.46/-0.47

Table S5. Crystal data and structure refinement for **P1**, **P3** and **M3**.

	P1	**P3**	**M3**
CCDC number	2064515	2064518	2064520
Empirical formula	$C_{31}H_{19}BCl_3FN_2O_2$	$C_{39}H_{24}BCl_2FN_2O_2$	$C_{39}H_{24}BCl_2FN_2O_2$
Formula weight	587.64	653.31	653.31
Temperature/K	100.01(10)	100.00(10)	301.13(11)
Crystal system	monoclinic	monoclinic	monoclinic
Space group	$P2_1$	$P2_1$	$P2_1$
a/Å	10.6816(3)	13.0101(4)	13.1863(4)
b/Å	20.2007(5)	10.3606(2)	10.3824(2)
c/Å	12.8842(3)	13.4292(4)	13.6545(5)
α/°	90	90	90
β/°	104.368(2)	118.414(4)	118.391(5)
γ/°	90	90	90
Volume/Å^3	2693.14(12)	1592.10(9)	1644.54(11)
Z	4	2	2
ρ_{calc}g/cm^3	1.449	1.363	1.319
μ/mm^{-1}	3.418	2.198	2.128
F(000)	1200.0	672.0	672.0
Crystal size/mm^3	0.2 × 0.2 × 0.1	0.15 × 0.05 × 0.01	0.3 × 0.15 × 0.03
Radiation	CuKα (λ = 1.54184)	CuKα (λ = 1.54184)	CuKα (λ = 1.54184)
2Θ range for data collection/°	7.082 to 144.048	7.484 to 151.862	7.36 to 151.794
Index ranges	-13 ≤ h ≤ 12, -24 ≤ k ≤ 18, -15 ≤ l ≤ 15	-15 ≤ h ≤ 16, -7 ≤ k ≤ 12, -16 ≤ l ≤ 16	-16 ≤ h ≤ 16, -12 ≤ k ≤ 10, -15 ≤ l ≤ 17
Reflections collected	10769	10899	12505
Independent reflections	7161 [R_{int} = 0.0285, R_{sigma} = 0.0451]	4690 [R_{int} = 0.0325, R_{sigma} = 0.0380]	5178 [R_{int} = 0.0441, R_{sigma} = 0.0516]
Data/restraints/parameters	7161/1/723	4690/1/426	5178/1/426
Goodness-of-fit on F^2	1.070	1.033	1.034
Final R indexes [I>=2σ (I)]	R_1 = 0.0321, wR_2 = 0.0768	R_1 = 0.0318, wR_2 = 0.0826	R_1 = 0.0396, wR_2 = 0.1021
Final R indexes [all data]	R_1 = 0.0363, wR_2 = 0.0798	R_1 = 0.0329, wR_2 = 0.0836	R_1 = 0.0457, wR_2 = 0.1063
Largest diff. peak/hole / e Å^{-3}	0.18/-0.22	0.21/-0.27	0.17/-0.25
Flack parameter	-0.004(11)	0.002(10)	0.032(13)

5. Photophysical data.

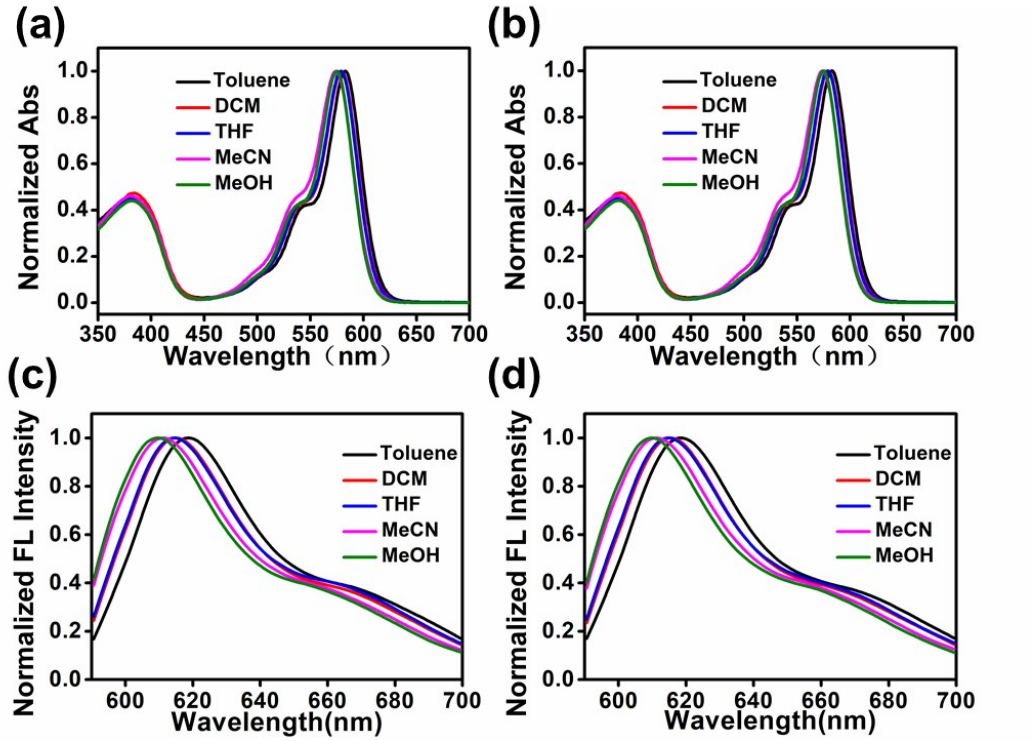

Fig. S6. The normalized absorption spectra of (a) **P1**, (b) **M1**, and the fluorescence spectra of (c) **P1**, (d) **M1** in different solvents.

Table S6. The maximum wavelengths of absorption and emission bands of **P1**/**M1** in different solvents.

	Toluene	DCM	THF	MeCN	MeOH		λ_{shift} [c] (nm)	λ_{shift} [c] (cm^{-1})
P1 λ_{abs} [a] (nm)	583	580	579	575	575	**P1 λ_{abs}**	8	238
M1 λ_{abs} [a] (nm)	583	580	579	575	575	**M1 λ_{abs}**	8	238
P1 λ_{em} [b] (nm)	619	615	615	611	610	**P1 λ_{em}**	9	238
M1 λ_{em} [b] (nm)	619	615	615	611	610	**M1 λ_{em}**	9	238

[a] Absorption maximum. [b] Fluorescence emission maxima. [c] The shift of absorption/emission bands in different solvents.

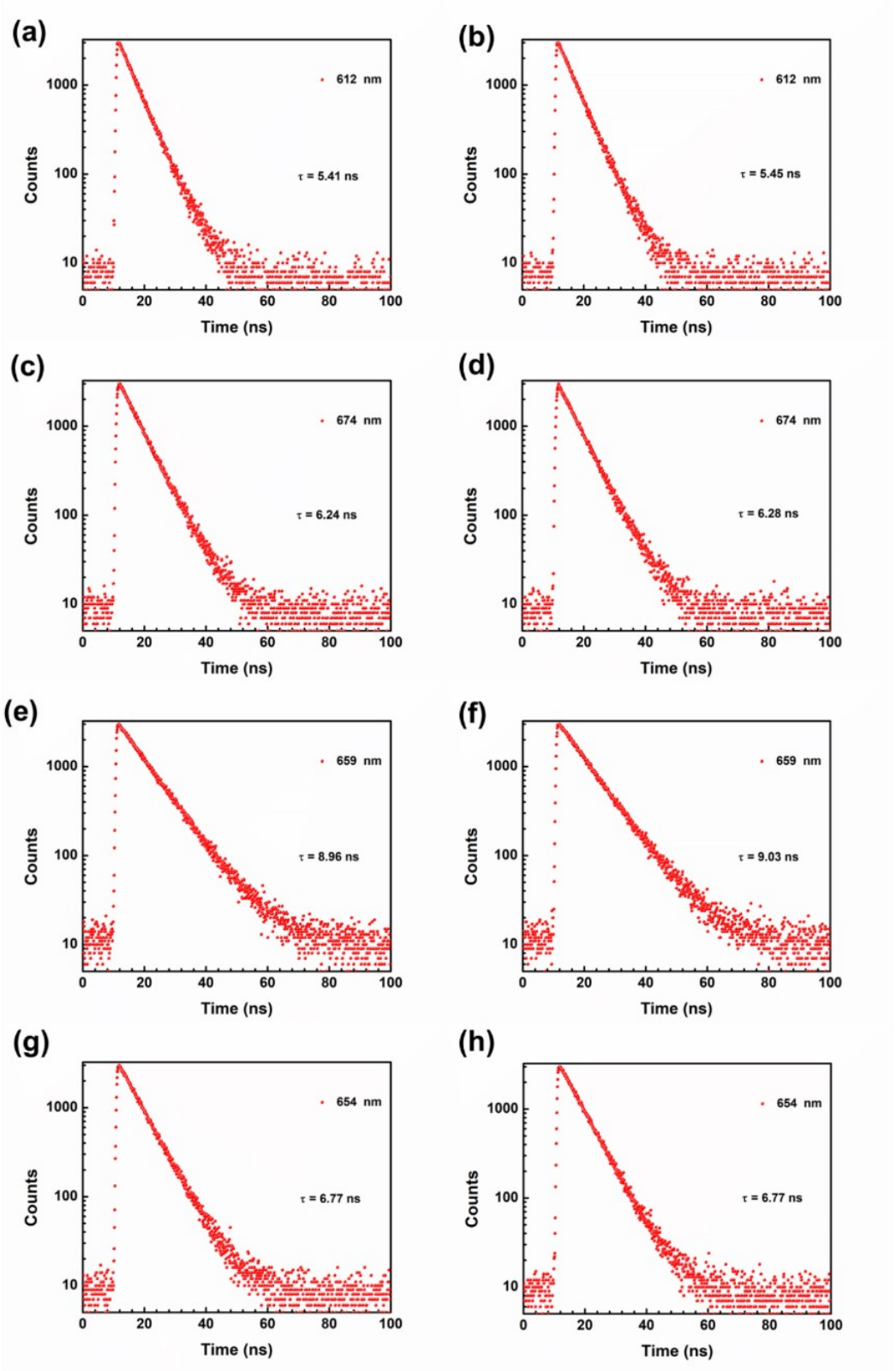

Fig. S7. Fluorescence decayed profiles of (a) **P1**. (b) **M1**. (c) **P2**. (d) **M2**. (e) **P3**. (f) **M3**. (g) **P4**. (h) **M4**. (monitored at maximum emission band)

Table S7. Photophysical data of all compounds **P1-P4/M1-M4** in dichloromethane solution.

	P1	**M1**	**P2**	**M2**	**P3**	**M3**	**P4**	**M4**
λ_{abs} [a] **(nm)**	580	580	619	619	619	619	619	619
ε [b] **($cm^{-1}M^{-1}$)**	53600	55300	41000	42000	42200	42900	56000	57600
λ_{em} [c] **(nm)**	615	615	674	674	659	659	654	654
$\Delta\nu$ [d] **(cm^{-1})**	981	981	1318	1318	981	981	865	865
Φ_f [e]	0.50	0.46	0.38	0.40	0.67	0.68	0.52	0.51
τ_f [f] **(ns)**	5.41	5.45	6.24	6.28	8.96	9.03	6.77	6.77
$\Delta\varepsilon$ [g] **($cm^{-1}M^{-1}$)**	36.1	-38.8	30.1	-34.9	33.5	-37.5	36.9	-33.5
g_{abs}*10^{-4} [h]	6.7	-7.0	7.3	-8.3	7.9	-8.7	6.6	-5.8
g_{lum} *10^{-4} [i]	+3.9	-3.4	+9.1	-9.6	+8.2	-6.0	+4.0	-2.3
B_{CPL} [j] **($M^{-1}cm^{-1}$)**	5.2	4.3	7.1	8.1	11.6	8.8	5.8	3.4
g_{lum}/ g_{abs}	0.58	0.48	1.24	1.15	1.03	0.69	0.61	0.40

[a] Absorption maximum. [b] Extinction coefficients calculated at the absorption maxima. [c] Fluorescence emission maxima. [d] Stoke shifts, Δν, were calculated by using the equation $1/\lambda_{abs} - 1/\lambda_{em}$. [e] Absolute fluorescence quantum yields. [f] Fluorescence lifetimes were measured with a λ=375 nm EPLEDs (picosecond-pulsed LEDs) light source and monitored at the emission maximum. All fluorescence lifetimes were fitted with single-exponential decays unless indicated. [g] Molar CD calculated at the absorption maxima. [h] The magnitude of CD can be quantified by the absorptive dissymmetry factor (g_{abs}), which is the ratio of molar CD to molar extinction coefficient [for unpolarized light $g_{abs} = \Delta\varepsilon/\varepsilon$]. [i] The degree of dissymmetry of CPL is quantified by the relative intensity difference of left and right circularly polarized emission which is called the luminescence dissymmetry factor. [j] The brightness for CPL defined as $B_{CPL} = \varepsilon \times \Phi \times g_{lum}/2$.

6. DFT calculation

All calculations were carried out with the GAUSSIAN16[3] quantum chemistry package based on (B3LYP/6-31g(d,p)).

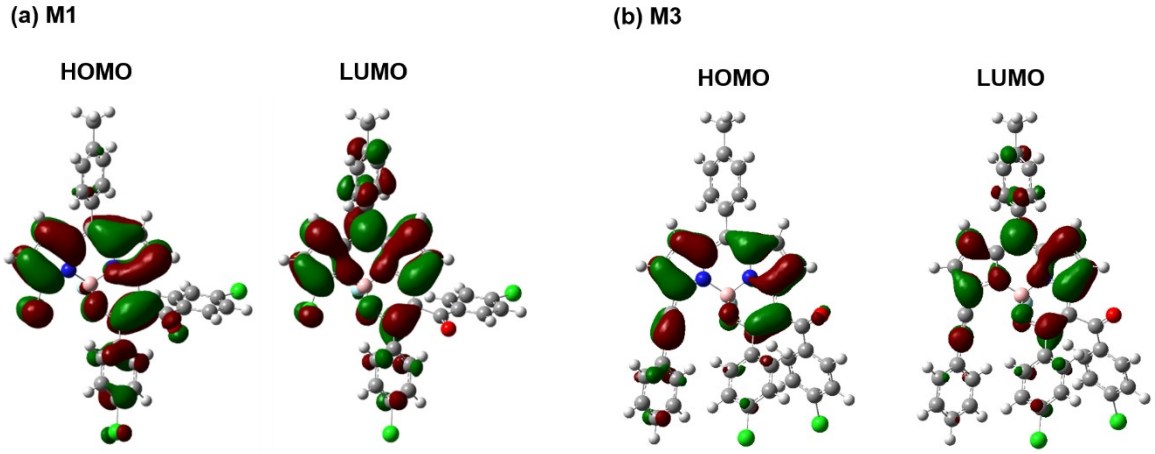

Fig. S8. HOMO/LUMO orbitals of (a) **M1** and (a) **M3** based on DFT calculations.

Table S8. The electric dipole moments (***μ***) and magnetic dipole moments (***m***) of the transition from S_1 to S_0 of **M1** and **M3** based on TD-DFT calculations.

M1

$\lvert\boldsymbol{\mu}\rvert$ (A.U.)			
x	y	z	total
2.9491	0.7243	0.4618	9.4351
$\lvert\boldsymbol{m}\rvert$ (A.U.)			
x	y	z	total
0.0528	0.5580	1.4674	2.4674

M3

$\lvert\boldsymbol{\mu}\rvert$ (A.U.)			
x	y	z	total
0.8252	-2.0560	-0.6724	5.3605
$\lvert\boldsymbol{m}\rvert$ (A.U.)			
x	y	z	total
-0.0270	0.4999	-2.8480	8.3617

7. Preparation of P1/M1 and P3/M3 assemblies.

The nanostructures were prepared according to our previous works. [4,5]

P1-NP/M1-NP: Stock THF solutions of **P1/M1** with the concentration of 1 mM were prepared, then inject the 0.5 mL stock solution into 2.5 mL stirring aqueous solution.

P1-SDS/M1-SDS: Stock THF solutions of **P1/M1** with the concentration of 1 mM were prepared, then inject the 0.5 mL stock solution into 2.5 mL stirring 2 mg/mL SDS aqueous solution.

P3-Solid/M3-Solid: Stock THF solutions of **P3/M3** with the concentration of 1 mM were prepared, then inject the 0.5 mL stock solution into 2.5 mL stirring aqueous solution.

P3-SDS/M3-SDS: Stock THF solutions of **P3/M3** with the concentration of 1 mM were prepared, then inject the 0.5 mL stock solution into 2.5 mL stirring 2 mg/mL SDS aqueous solution.

The surfactant served as solubilizer and template directing the formation of nanocrystals. The surfactant stabilized the aggregates and induced the growth of the nanocrystals by selectively adhere on a certain facet and slow down the grow rate of that facet compared with the others, leading to the formation of nanocrystals. Compound structure also plays important roles for forming nanocrystals. **P1/M1** did not form nanocrystals even in the presence of SDS probably due to the less crystallinity compared to **P3/M3**.

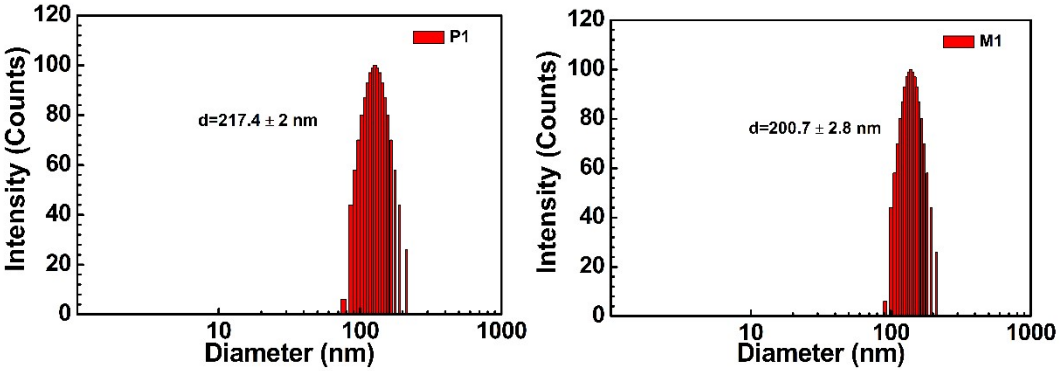

Fig. S9. The diameter of **P1-NP** and **M1-NP** measured using DLS.

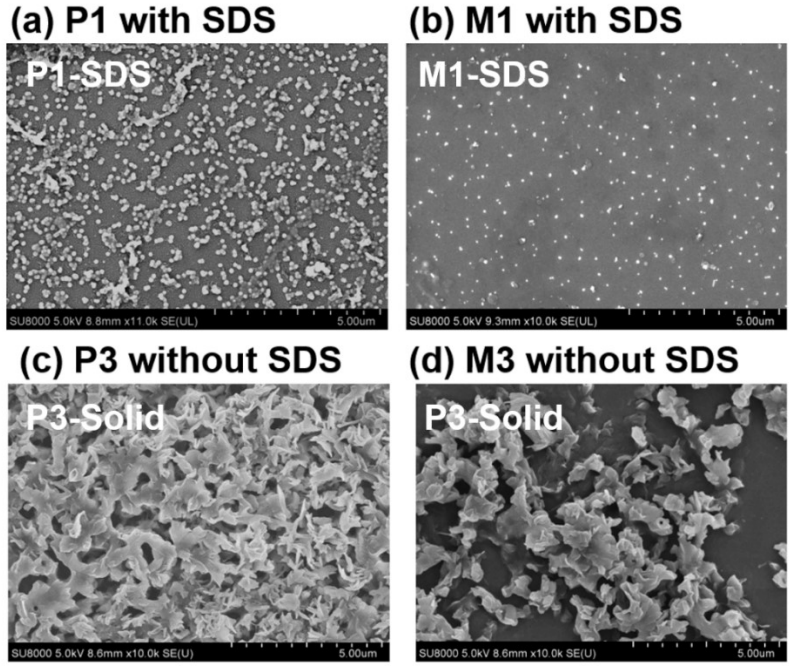

Fig. S10. SEM images of (a) **P1-SDS**, (b) **M1-SDS**, (c) **P3-Solid** and (d) **M3-Solid**.

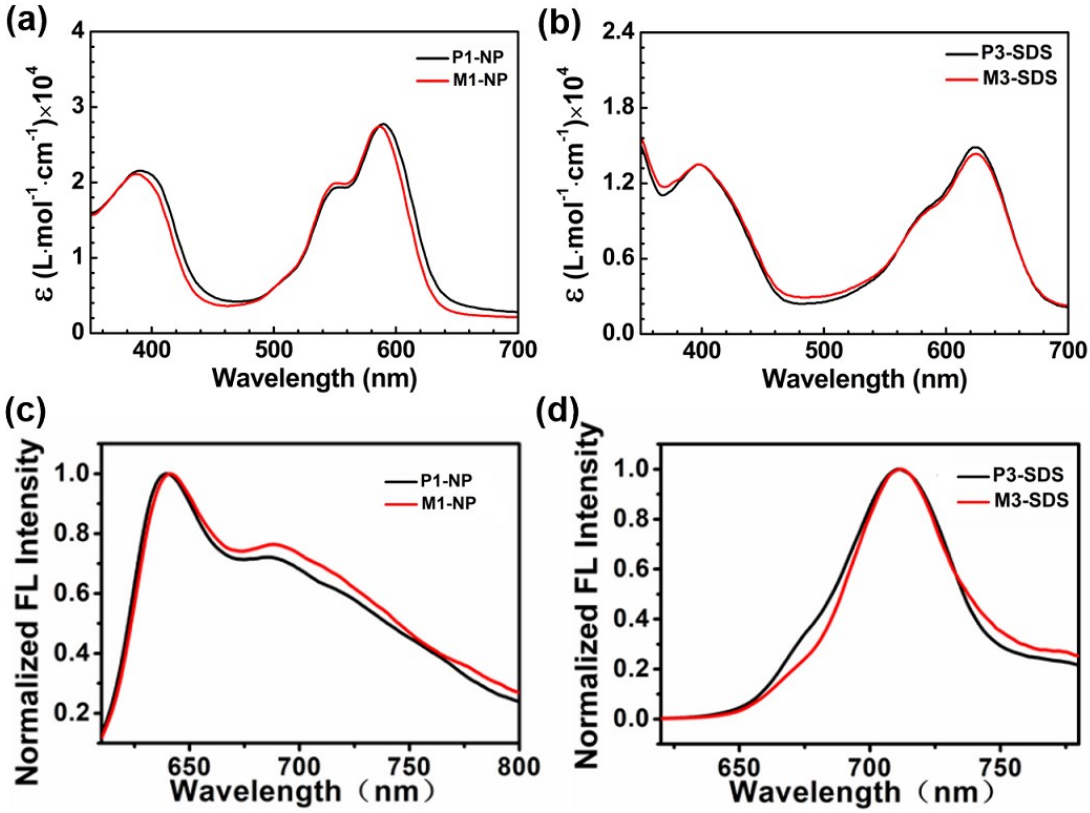

Fig. S11. The absorption spectra of (a) **P1-NP/M1-NP** and (b) **P3-SDS/M3-SDS.** The fluorescence spectra of (c) **P1-NP/M1-NP** and (d) **P3-SDS/M3-SDS**.

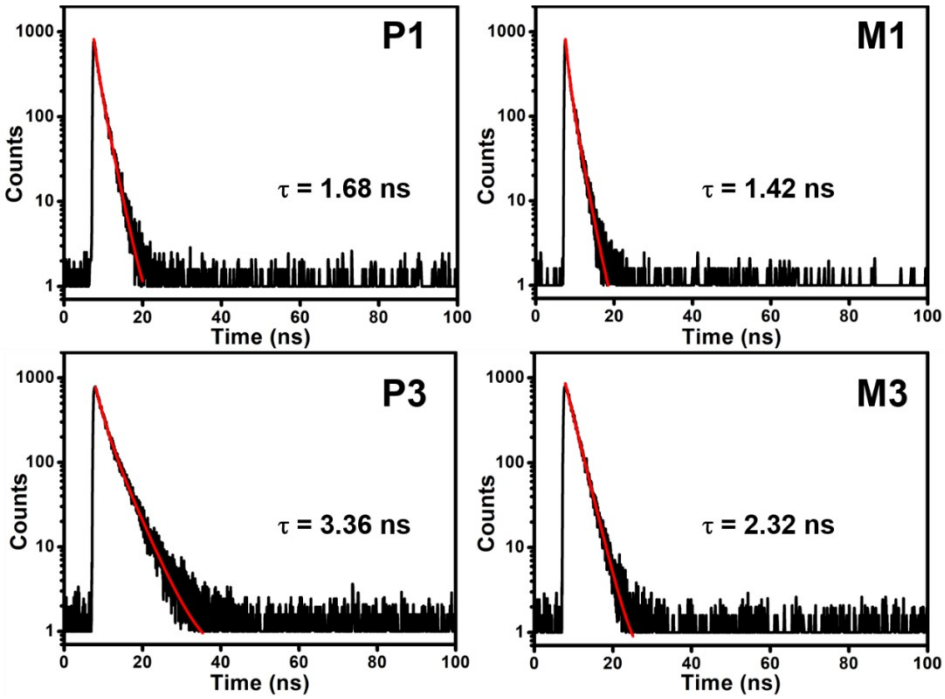

Fig. S12. Fluorescence decayed profiles of **P1-NP**/**M1-NP** and **P3-SDS**/**M3-SDS**.

Table S9. Comparison of photophysical data of compounds **P1**/**M1** and **P3**/**M3** in solutions and in solid states.

	λ_{em} (nm) [c]	Φ (%) [d]	τ (ns) [e]	K_r (10^7 s^{-1}) [f]	K_{nr} (10^7 s^{-1}) [g]
P1 [a]	615	50	5.41	9.2	9.2
P1-NP [b]	640	4.3	1.68	2.6	57
M1 [a]	615	46	5.45	8.4	9.9
M1-NP [b]	640	4.5	1.42	3.2	67
P3 [a]	659	67	8.96	7.5	3.68
P3-SDS [b]	710	11.2	3.36	3.3	26
M3 [a]	659	68	9.03	7.5	3.5
M3-SDS [b]	710	8.3	2.32	3.5	40

[a] Measured in DCM. [b] Measured in water. [c] Fluorescence emission maxima. [d]Absolute fluorescence quantum yields. [e] The lifetime of the fluorescence. [f] Radiative decay rate, $k_r = \Phi/\tau$. [g] Non-radiative decay rate, $k_{nr} = (1-\Phi)/\tau$.

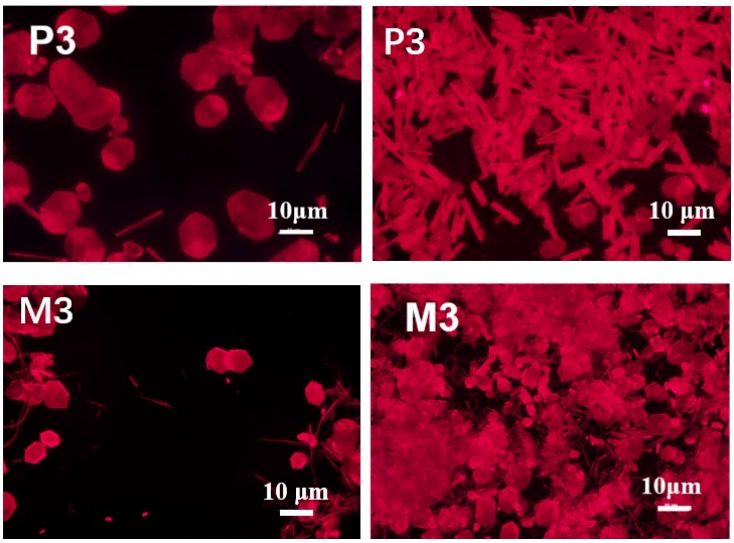

Fig. S13. Fluorescence microscopy images of **P3-SDS/M3-SDS**.

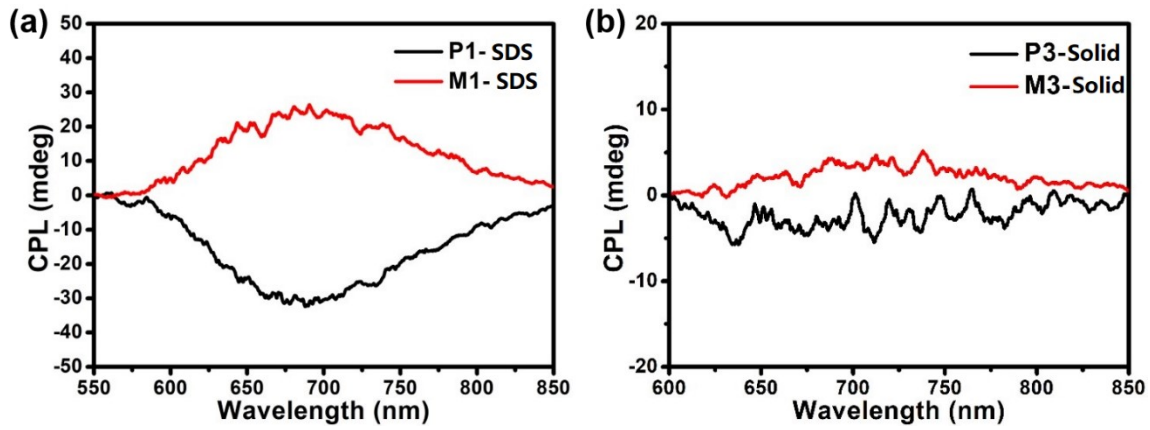

Fig. S14. CPL spectra of (a) **P1-SDS/M1-SDS** and (b) **P3-Solid/M3-Solid.**

8. NMR and mass spectra of compounds P1-P4/M1-M4.

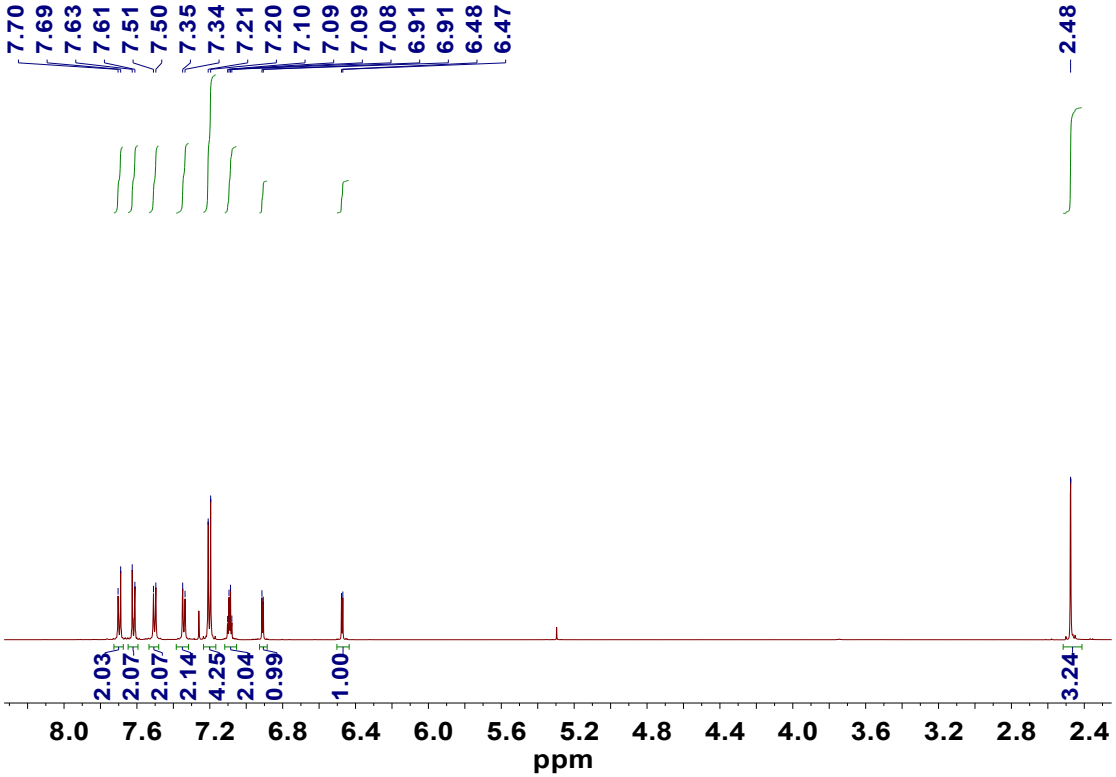

Fig. S15. ^{1}H NMR spectrum of **P1** in $CDCl_3$

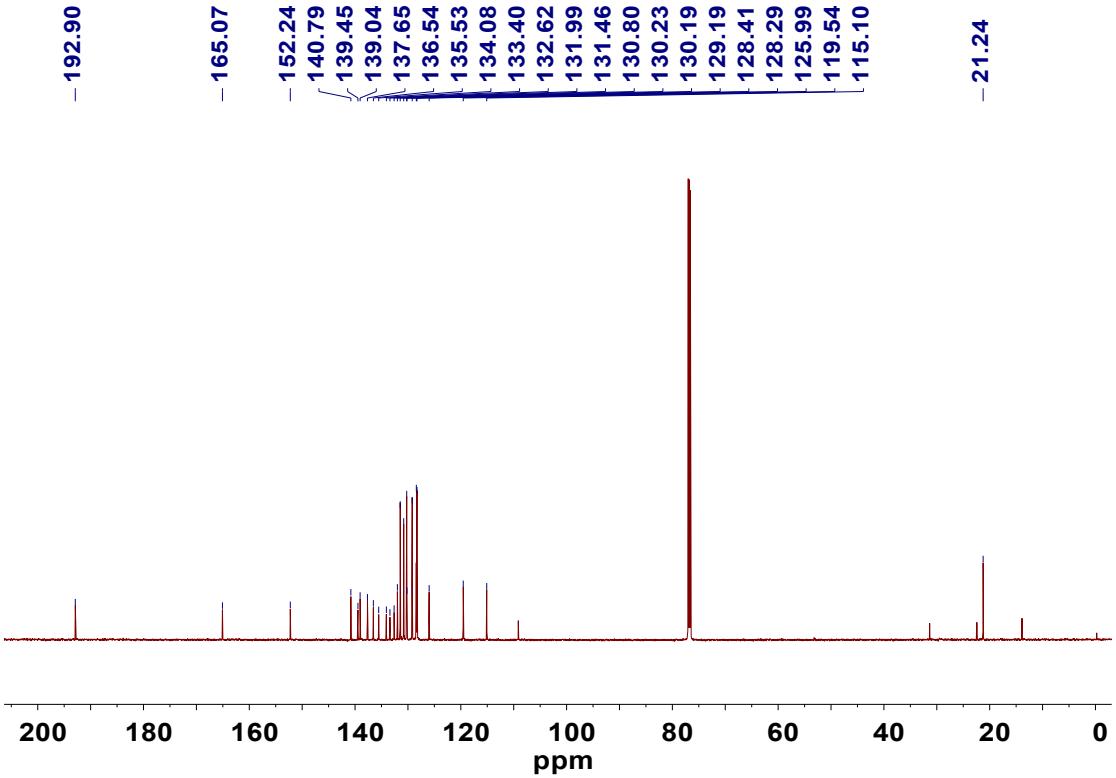

Fig. S16. ^{13}C NMR spectrum of **P1** in $CDCl_3$

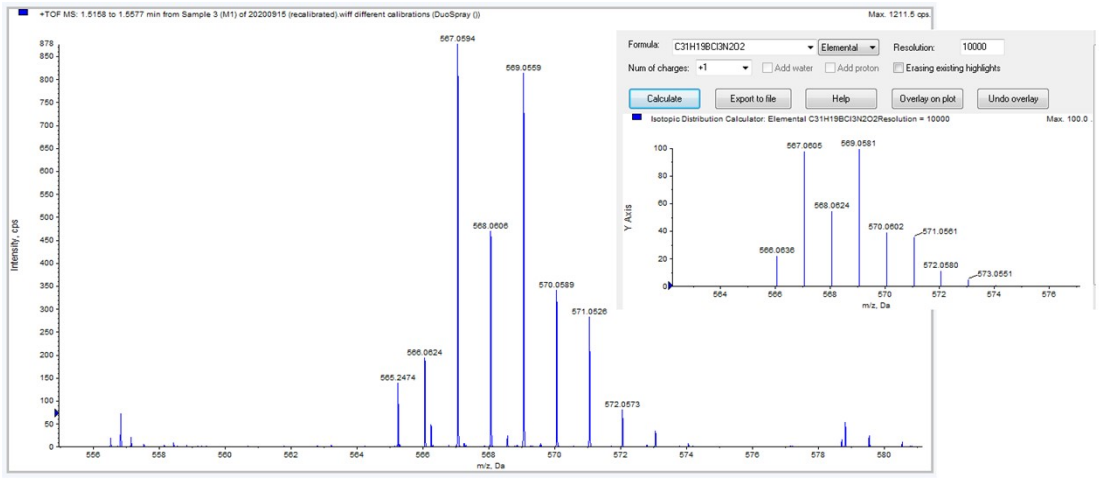

Fig. S17. Mass spectrum of **P1.**

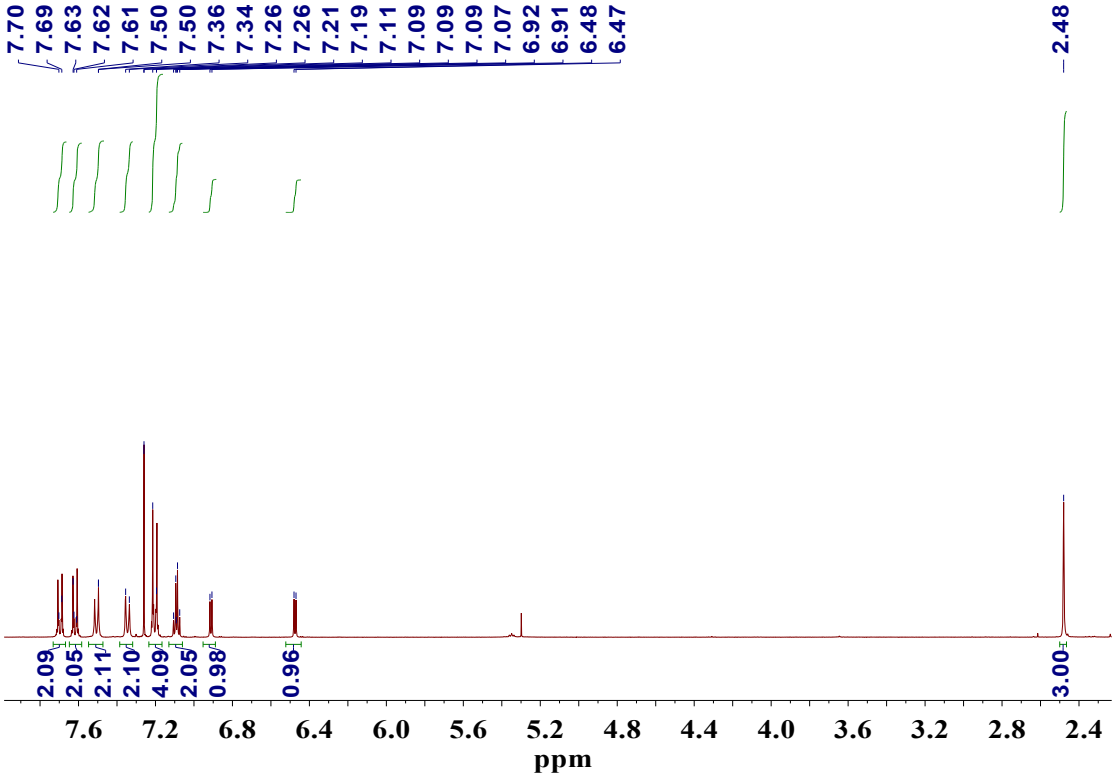

Fig. S18. ^{1}H NMR spectrum of **M1** in $CDCl_3$

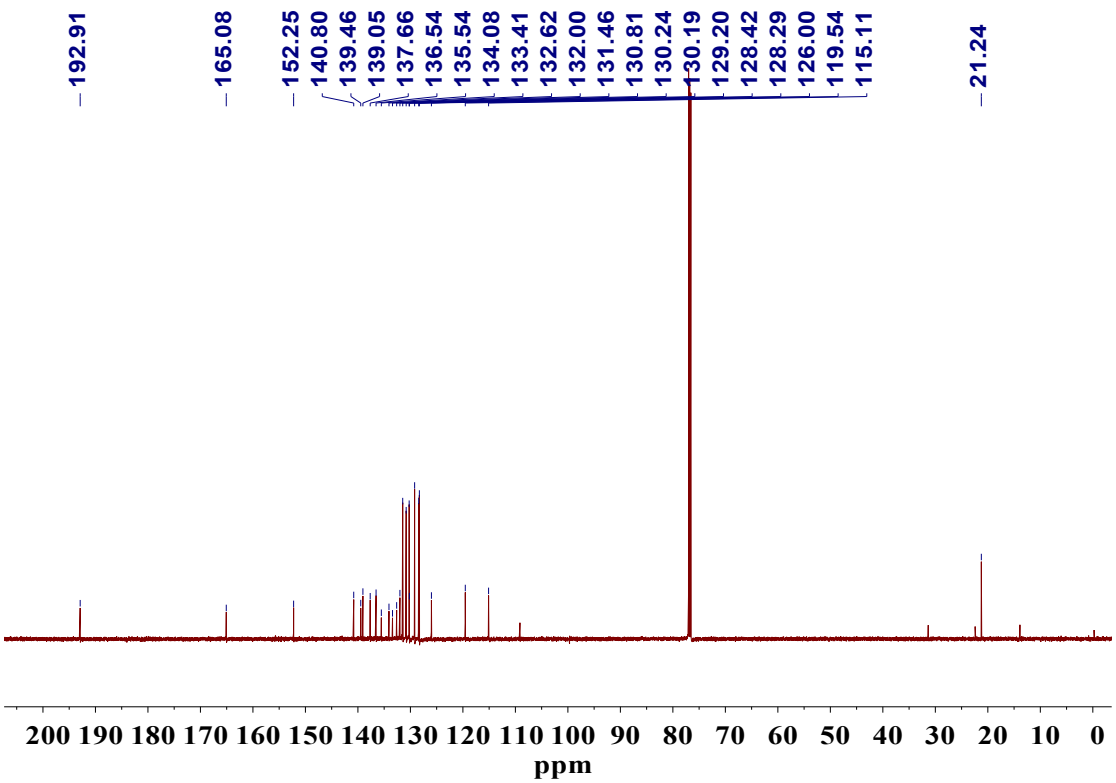

Fig. S19. ^{13}C NMR spectrum of **M1** in $CDCl_3$

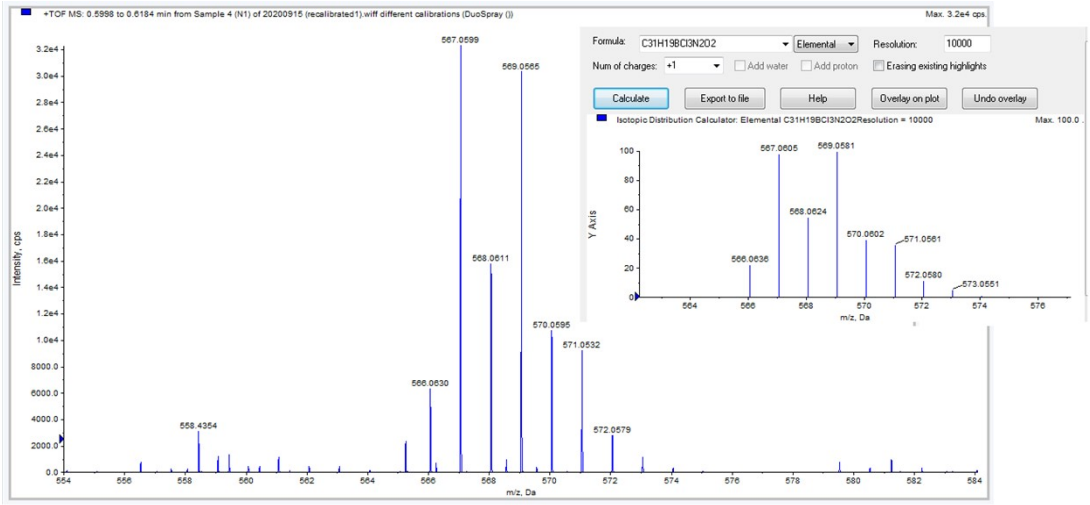

Fig. S20. Mass spectrum of **M1**

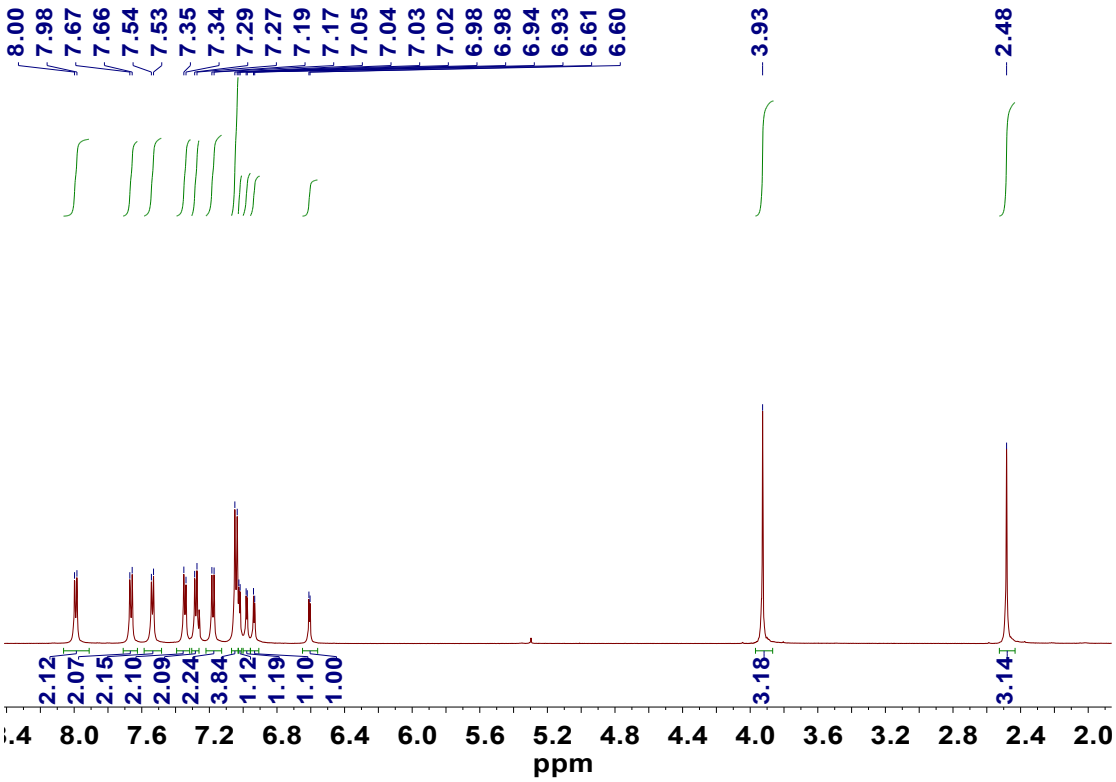

Fig. S21. ^{1}H NMR spectrum of **P2** in $CDCl_3$

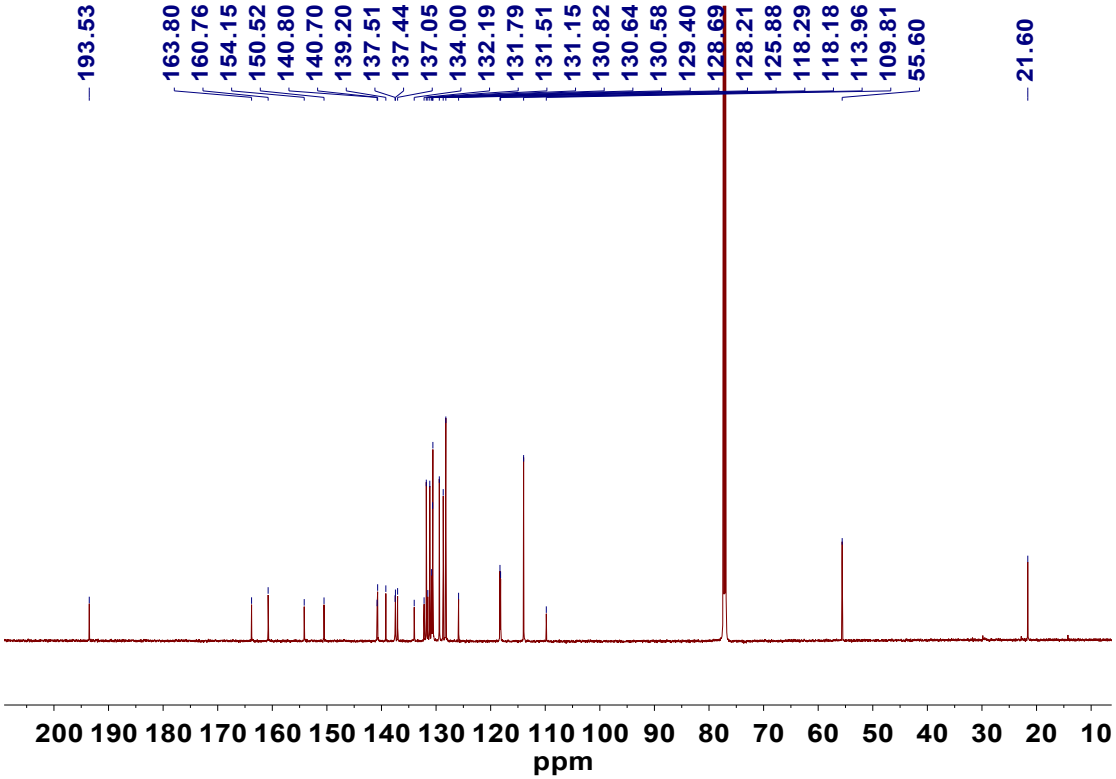

Fig. S22. ^{13}C NMR spectrum of **P2** in $CDCl_3$

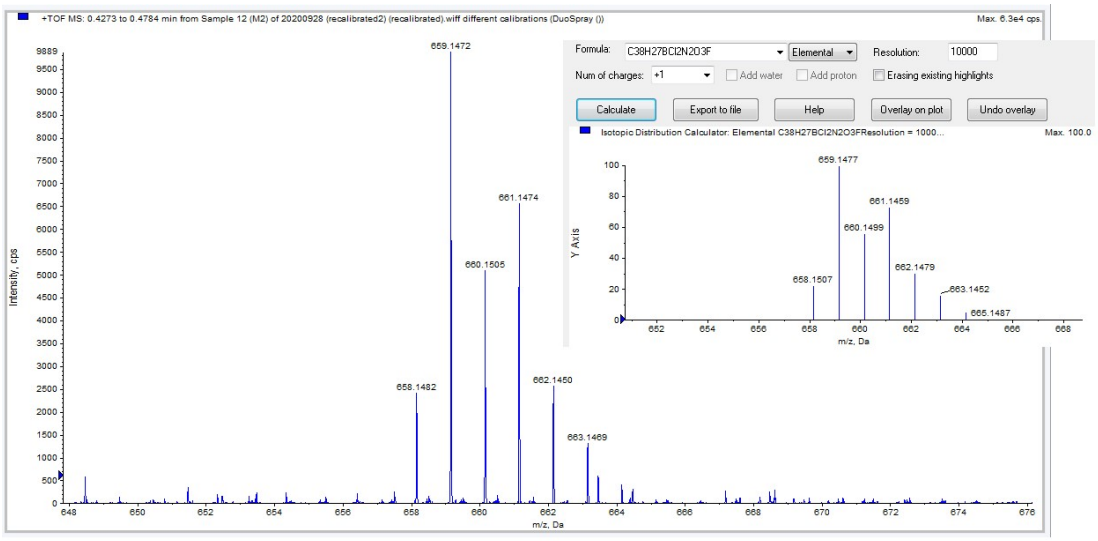

Fig. S23. Mass spectrum of **P2**

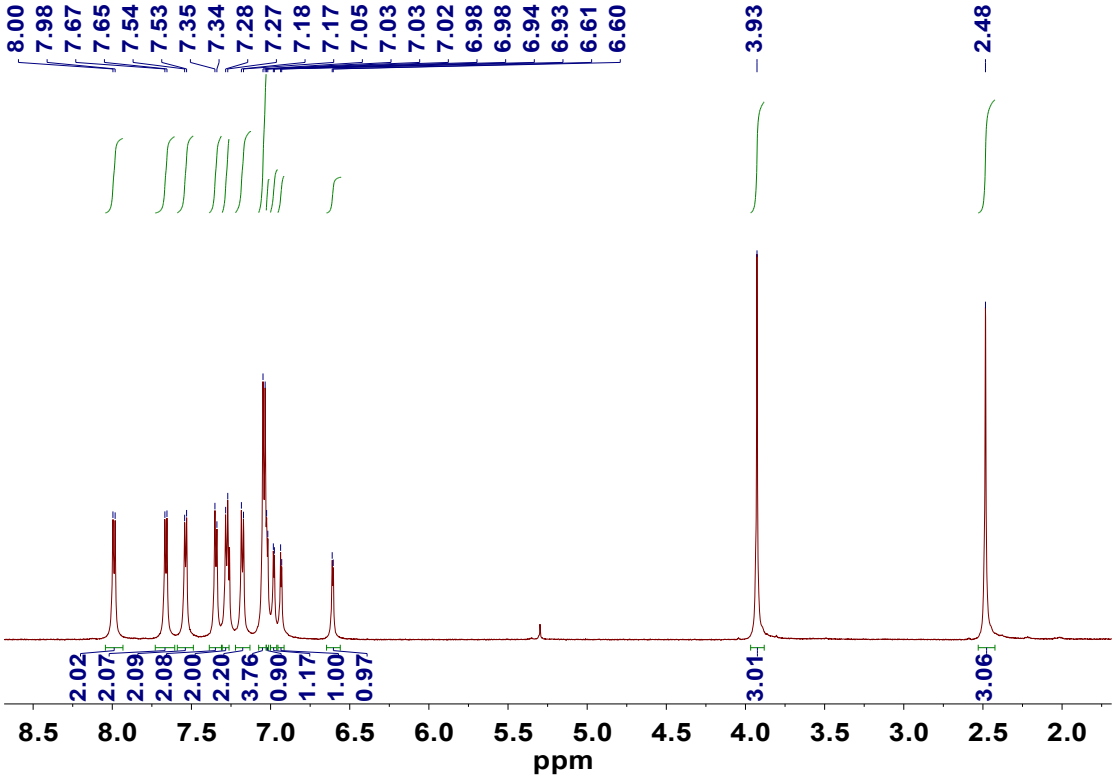

Fig. S24. ^{1}H NMR spectrum of **M2** in $CDCl_3$

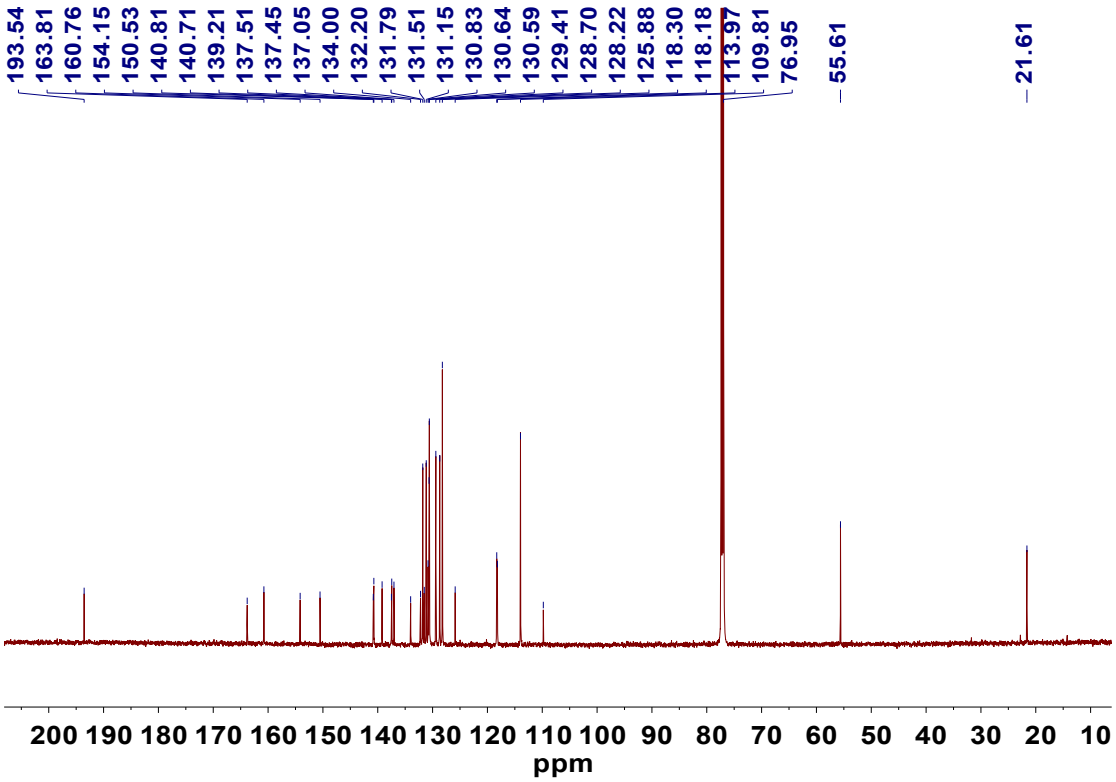

Fig. S25. ^{13}C NMR spectrum of **M2** in $CDCl_3$

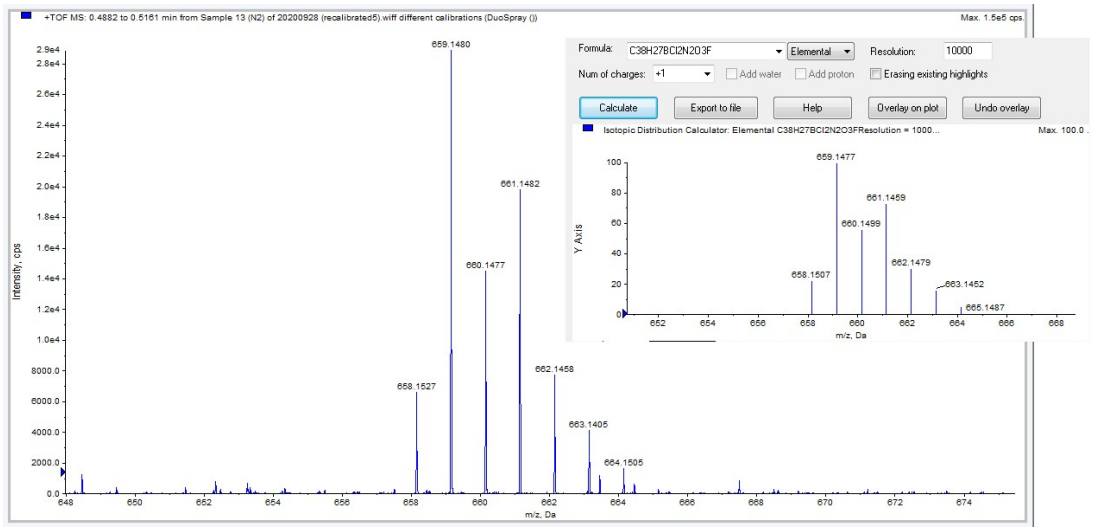

Fig. S26. Mass spectrum of **M2**

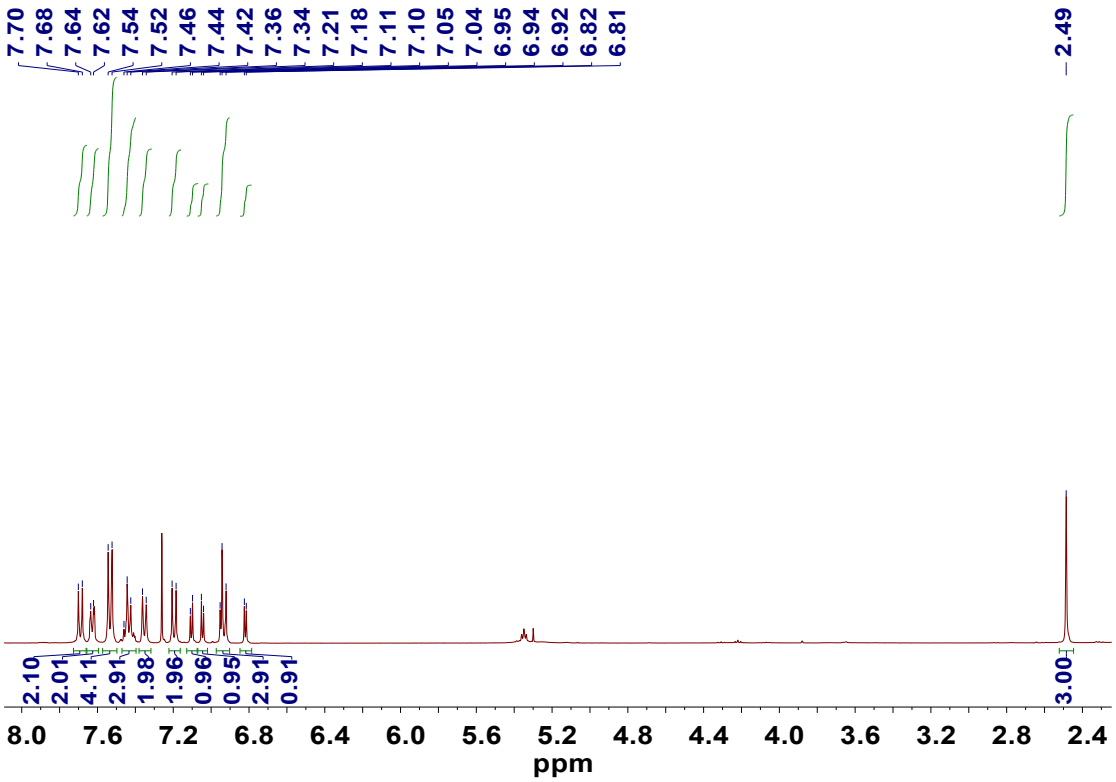

Fig. S27. ^{1}H NMR spectrum of **P3** in $CDCl_3$

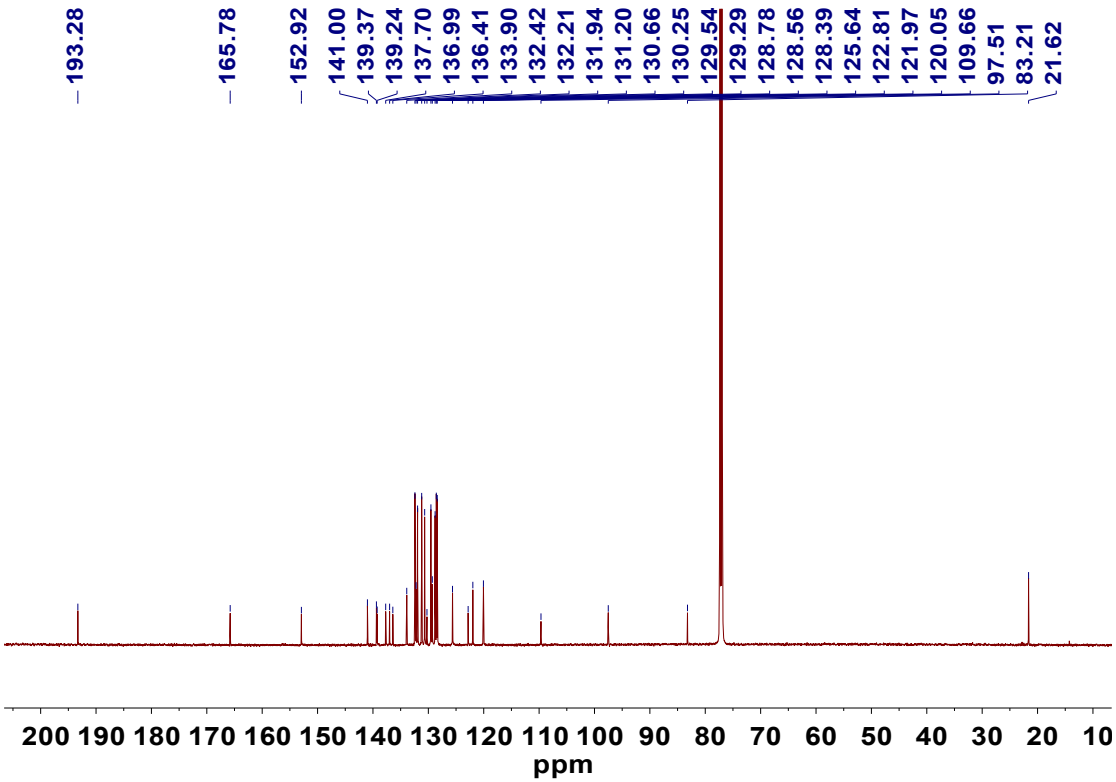

Fig. S28. ^{13}C NMR spectrum of **P3** in $CDCl_3$

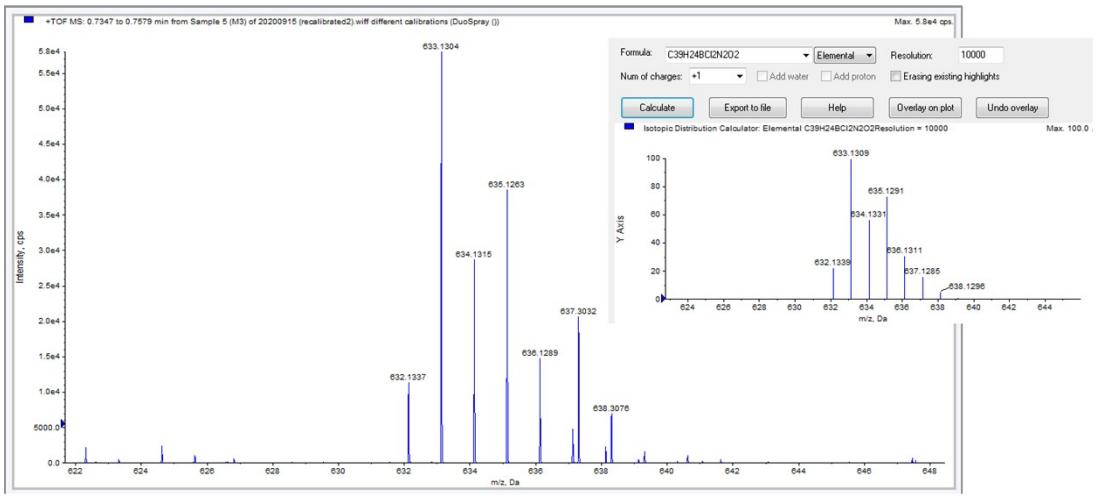

Fig. S29. Mass spectrum of **P3**

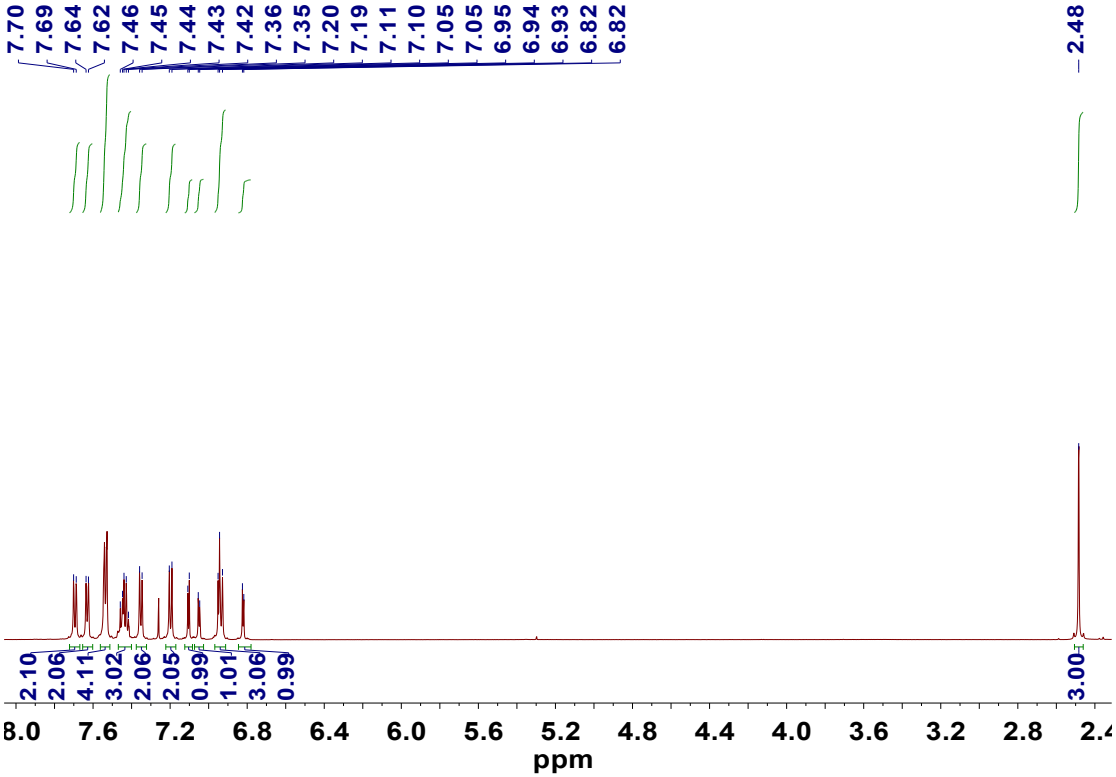

Fig. S30. ^{1}H NMR spectrum of **M3** in $CDCl_3$

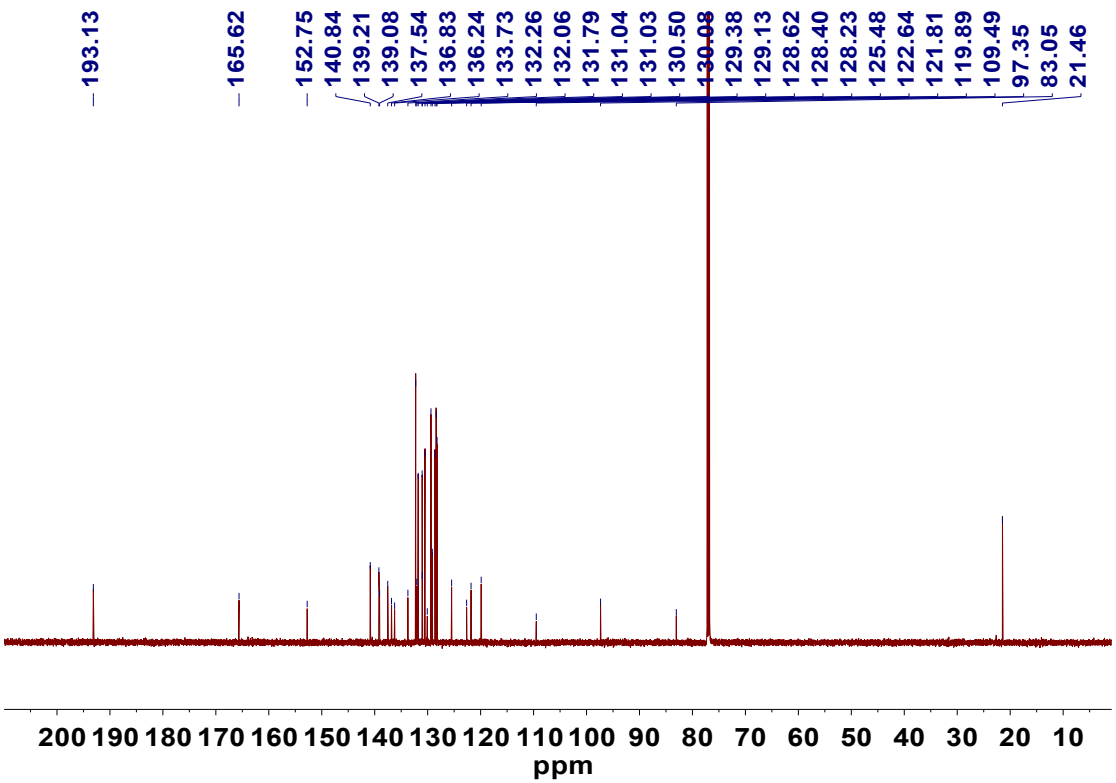

Fig. S31. ^{13}C NMR spectrum of **M3** in $CDCl_3$

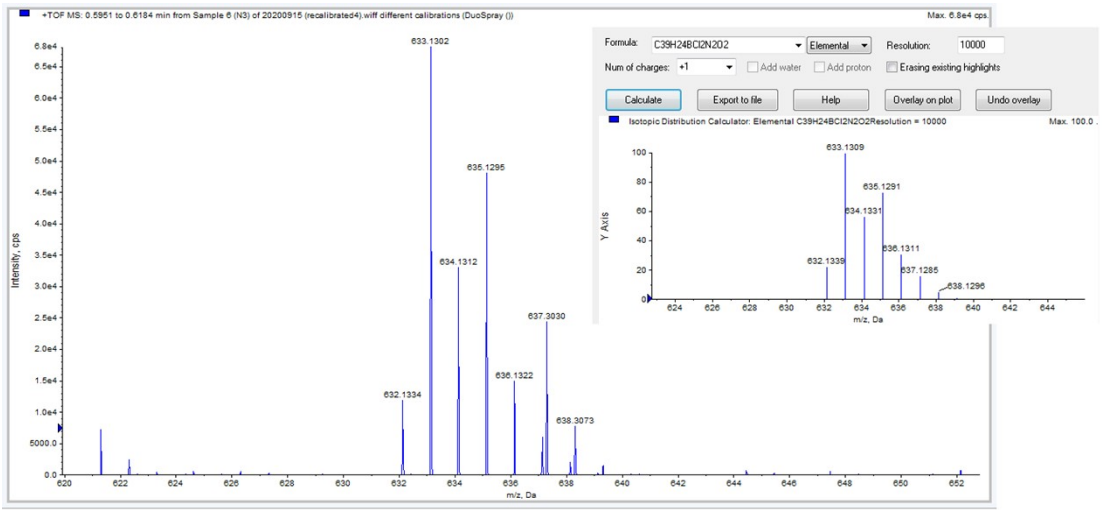

Fig. S32. Mass spectrum of **M3**

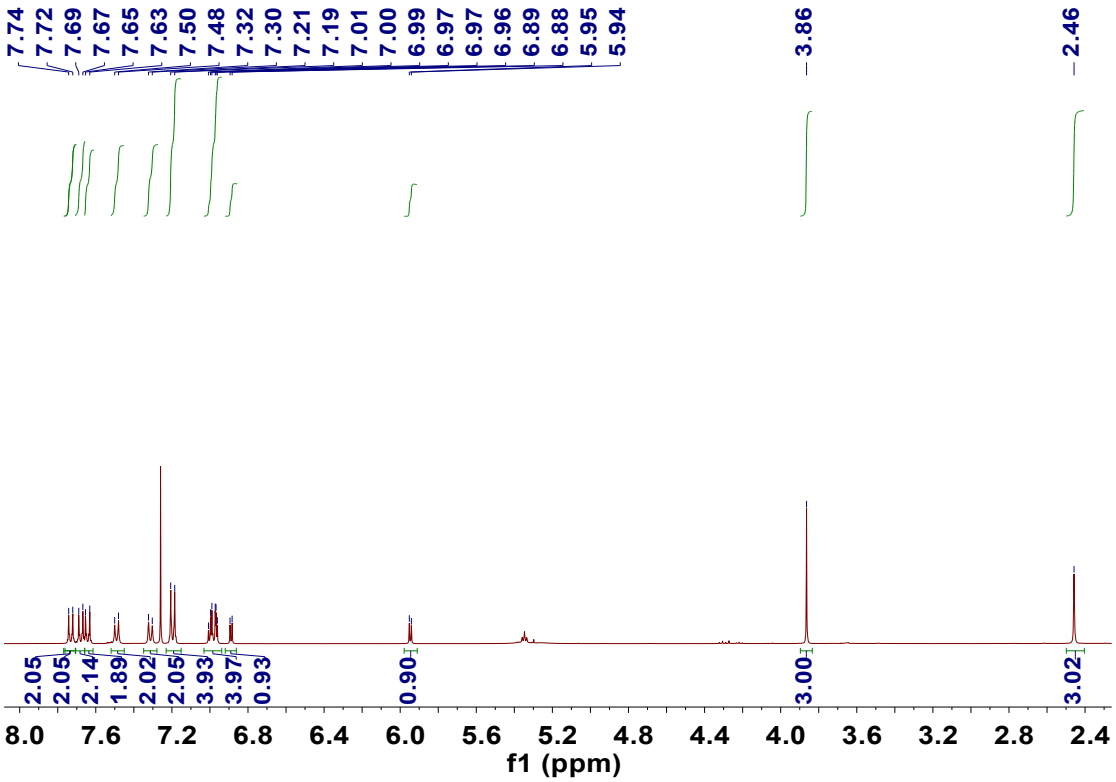

Fig. S33. ^{1}H NMR spectrum of **P4** in $CDCl_3$

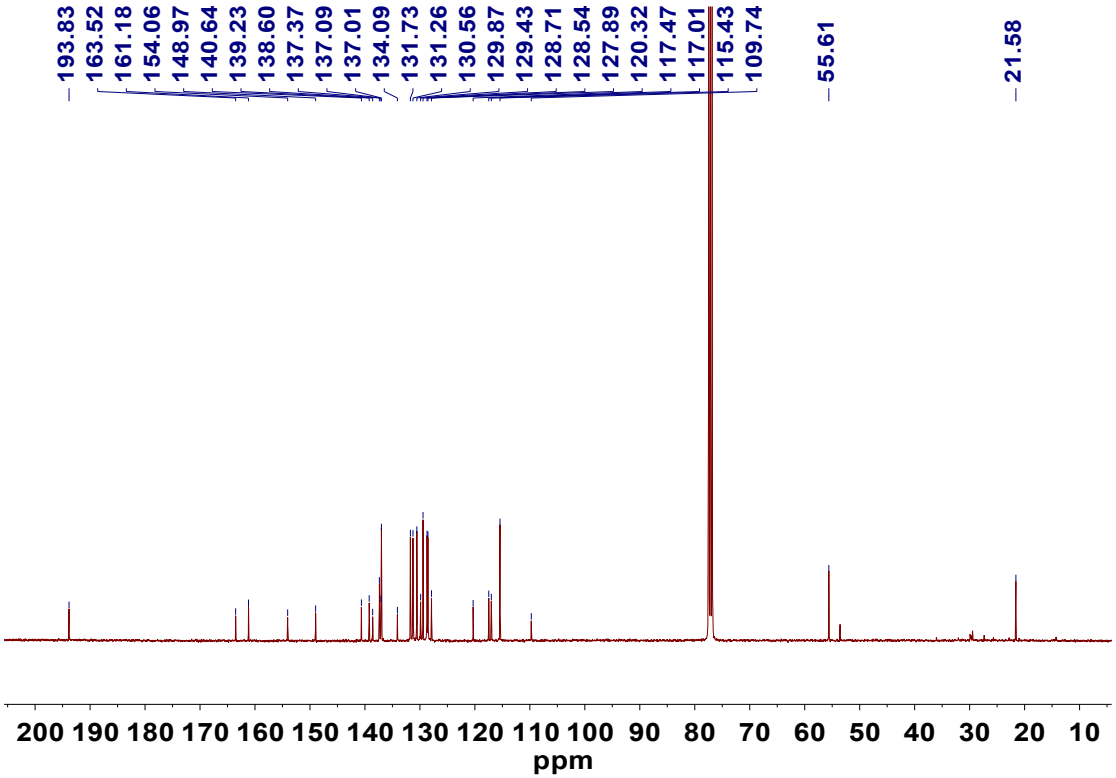

Fig. S34. ^{13}C NMR spectrum of **P4** in $CDCl_3$

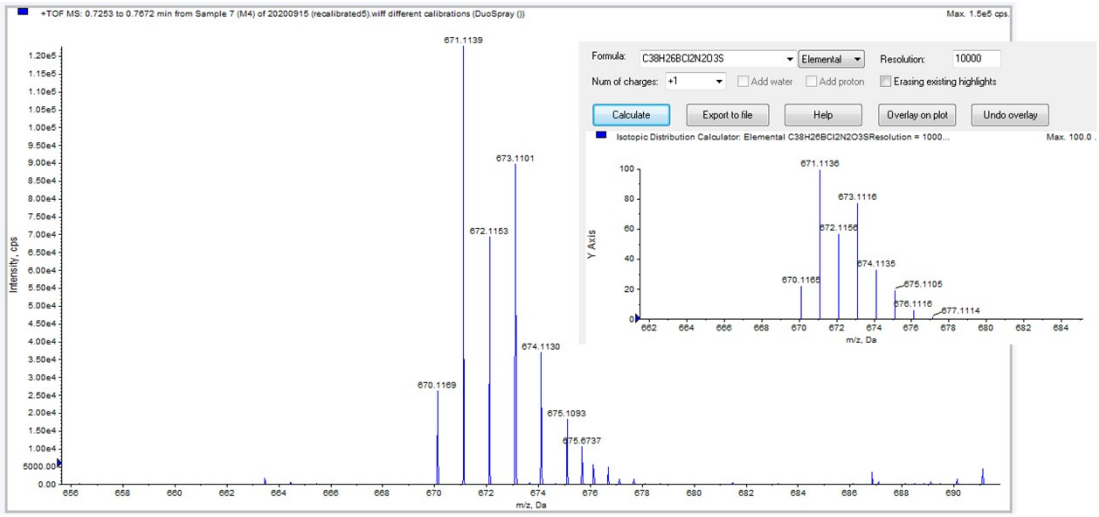

Fig. S35. Mass spectrum of **P4**

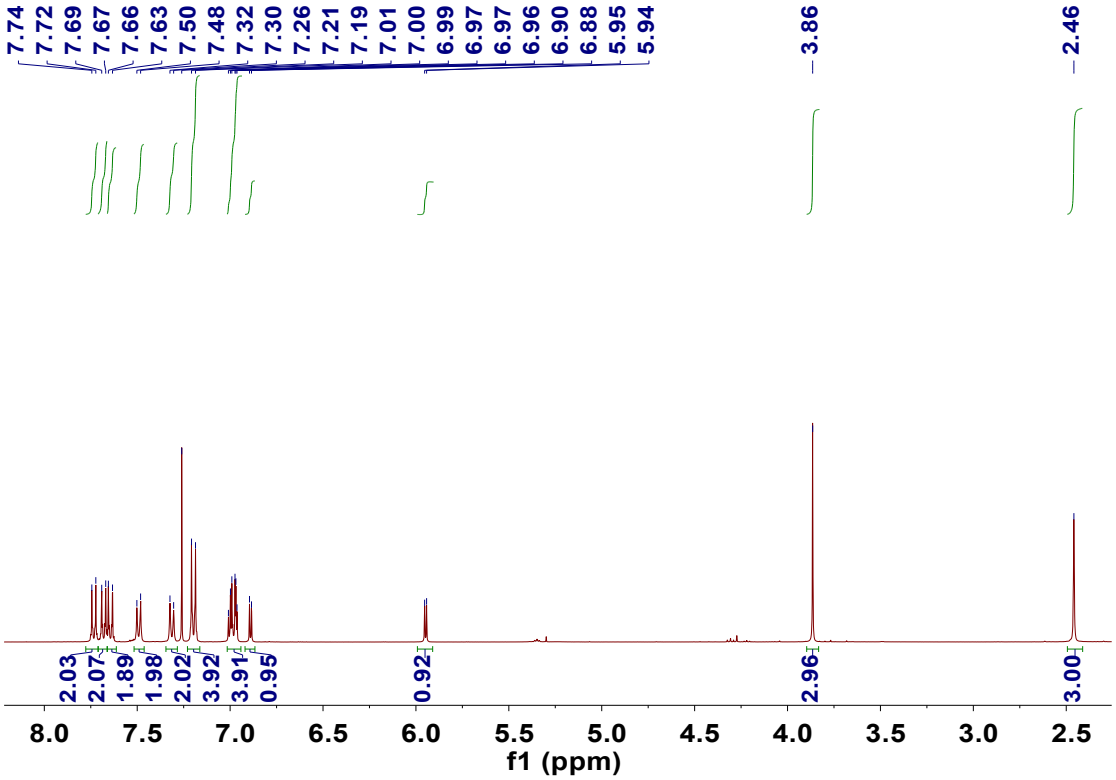

Fig. S36. ^{1}H NMR spectrum of **M4** in $CDCl_3$

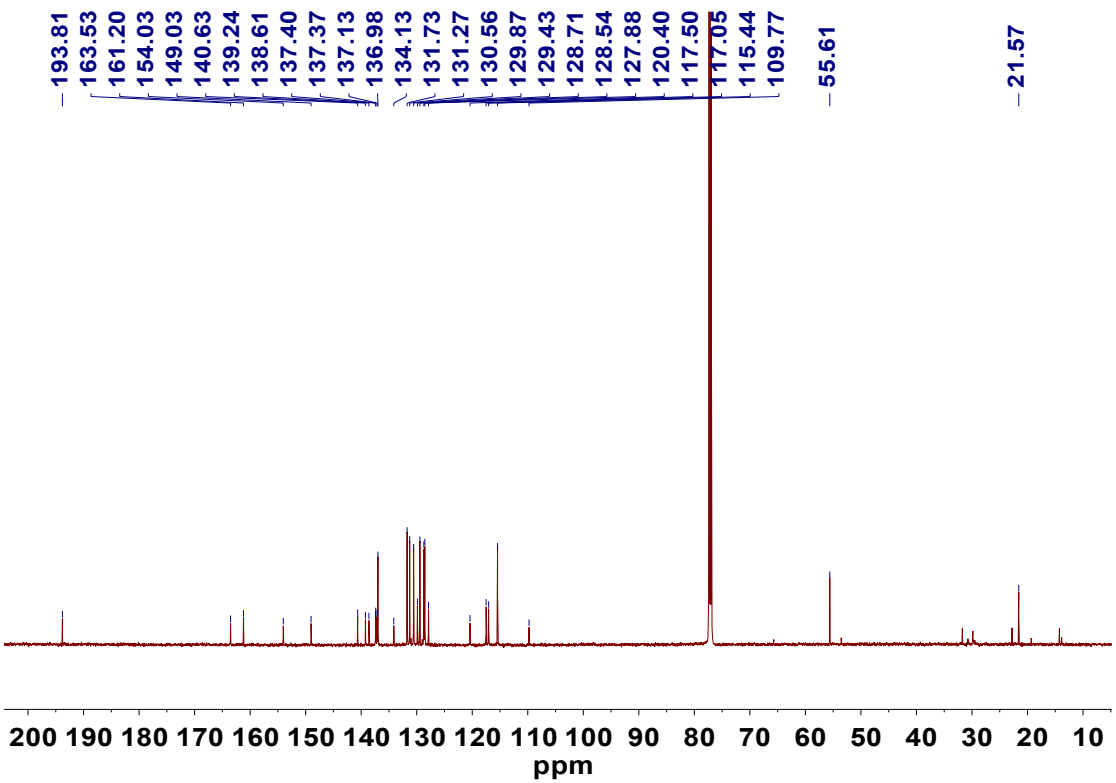

Fig. S37. ^{13}C NMR spectrum of **M4** in $CDCl_3$

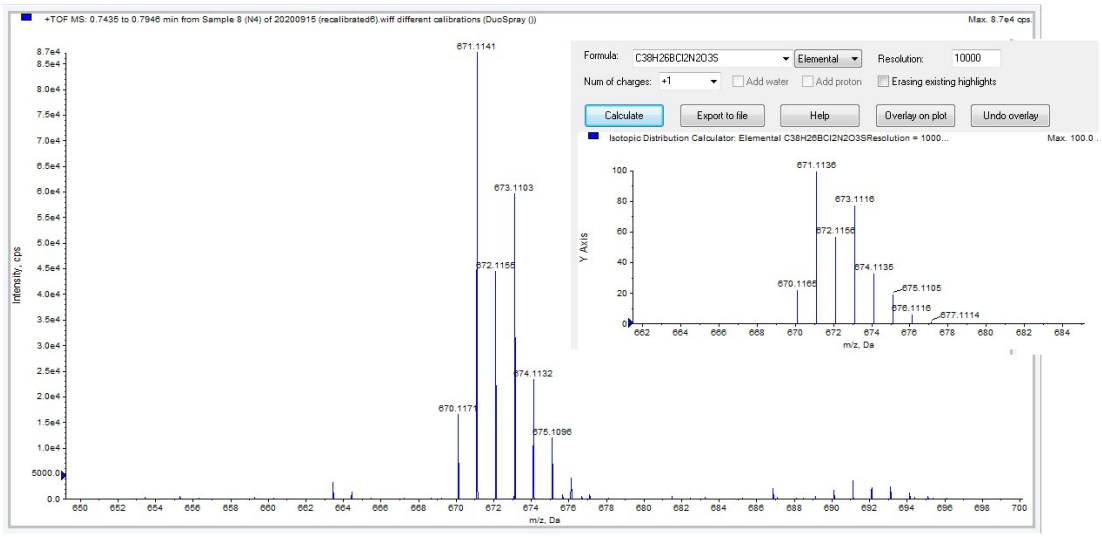

Fig. S38. Mass spectrum of **M4**

9. Reference

[1] K. X. Teng, L. Y. Niu, J. Li, L. Jia, Q. Z. Yang, *Chem. Commun.* 2019**, 55**, 13761-13764.

[2] Y. Liu, L.-Y. Niu, X.-L. Liu, P.-Z. Chen, Y.-S. Yao, Y.-Z. Chen and Q.-Z. Yang, *Chem. Eur. J.*, 2018, **24**, 13549.

[3] Gaussian 16, Revision B.01, M. J. Frisch, G. W. Trucks, H. B. Schlegel, G. E. Scuseria, M. A. Robb, J. R. Cheeseman, G. Scalmani, V. Barone, G. A. Petersson, H. Nakatsuji, X. Li, M. Caricato, A. V. Marenich, J. Bloino, B. G. Janesko, R. Gomperts, B. Mennucci, H.

P. Hratchian, J. V. Ortiz, A. F. Izmaylov, J. L. Sonnenberg, D. Williams-Young, F. Ding, F. Lipparini, F. Egidi, J. Goings, B. Peng, A. Petrone, T. Henderson, D. Ranasinghe, V. G. Zakrzewski, J. Gao, N. Rega, G. Zheng, W. Liang, M. Hada, M. Ehara, K. Toyota, R. Fukuda, J. Hasegawa, M. Ishida, T. Nakajima, Y. Honda, O. Kitao, H. Nakai, T. Vreven, K. Throssell, J. A. Montgomery, Jr., J. E. Peralta, F. Ogliaro, M. J. Bearpark, J. J. Heyd, E. N. Brothers, K. N. Kudin, V. N. Staroverov, T. A. Keith, R. Kobayashi, J. Normand, K. Raghavachari, A. P. Rendell, J. C. Burant, S. S. Iyengar, J. Tomasi, M. Cossi, J. M. Millam, M. Klene, C. Adamo, R. Cammi, J. W. Ochterski, R. L. Martin, K. Morokuma, O. Farkas, J. B. Foresman, and D. J. Fox, Gaussian, Inc., Wallingford CT, 2016.

[4] P.-Z. Chen, L.-Y. Niu, H. Zhang, Y.-Z. Chen and Q.-Z. Yang, *Mater. Chem. Front.*, 2018, **2**, 1323.

[5] P. Z. Chen, Y. X. Weng, L. Y. Niu, Y. Z. Chen, L. Z. Wu, C. H. Tung and Q. Z. Yang, *Angew. Chem. Int. Ed.*, 2016, **55**, 2759.